Energy Conversion and Management 339 (2025) 119859

Contents lists available at ScienceDirect

Energy Conversion and Management

journal homepage: www.elsevier.com/locate/enconman

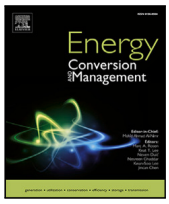

Research paper

Integrating organic Rankine cycles for waste heat recovery from onboard diesel generators in the maritime sector: Simulation and techno-economic assessment

Daniel Sánchez-Lozano [a], Roque Aguado [a,*], Antonio Escámez [a], José Antonio Hernández-Torres [b], Juan P. Torreglosa [b], David Vera [a]

[a] Departamento de Ingeniería Eléctrica, Escuela Politécnica Superior de Linares, Universidad de Jaén, Avda. de la Universidad s/n, 23700 Linares, Spain
[b] Departamento de Ingeniería Eléctrica y Térmica, de Diseño y Proyectos, Escuela Técnica Superior de Ingeniería, Universidad de Huelva, Avda. de las Fuerzas Armadas s/n, 21007 Huelva, Spain

ARTICLE INFO

Keywords:
Organic Rankine cycle
Waste heat recovery
Maritime sector
Hybrid electric propulsion
Working fluid selection
Sensitivity analysis

ABSTRACT

The maritime sector's dependence on fossil fuels, coupled with the rising crude oil prices, underscores the urgent need to enhance ship efficiency and advance the decarbonization of the marine sector. This paper evaluates the technical and economic feasibility of integrating organic Rankine cycle (ORC) systems in diesel-electric propulsion marine distribution vessels. A comprehensive simulation and optimization of a 1.6 MW ORC unit, using acetone as the working fluid, has been conducted. The system is designed to recover waste heat from the exhaust gases of diesel generators aboard a vessel. Under an 85% load of the diesel generators, the ORC bottoming unit demonstrates a net electrical efficiency of 8.45% with a thermodynamic cycle efficiency of 18.73%. It is estimated that this system could reduce annual carbon dioxide emissions and diesel fuel consumption by 18.5% compared to conventional systems. From a financial perspective, assuming a conservative discount rate of 8%, the ORC system demonstrates long-term viability with a cumulative profit of 44% on the initial investment, a payback period of 11.7 years, and an internal rate of return of 12.8%. Additionally, the advantages of integrating the ORC with direct current distribution networks are highlighted, simplifying system architecture and improving energy efficiency.

1. Introduction

The rising crude oil prices are motivating shipping industries to improve vessel efficiency and reduce their dependency on fossil fuels [1]. As the global gross domestic product grows, the maritime sector is experiencing an increase in energy demand [2]. According to estimates by the International Maritime Organization (IMO) [3], the shipping sector emitted a total of 1056 million tonnes of CO_2 in 2018, accounting for approximately 2.89% of anthropogenic CO_2 emissions. International shipping contributes to only about 9% of the global emissions related to the transport sector [3]. However, a 40%–115% growth is expected in the maritime trade sector by 2050 in comparison to 2020 levels [3]. Nowadays, approximately 99% of international shipping's energy demand is met by fossil fuels, with fuel oil and marine gas oil (MGO) accounting for up to 95% of the total demand [2]. Therefore, urgent action is imperative to accelerate the energy transformation, promote sustainability, and achieve decarbonization of the sector. Otherwise, the IMO warns that greenhouse gas (GHG) emissions associated with shipping could increase by 50%–250% by 2050 compared to 2008 emission levels [2]. The shipping industry is currently focusing on decarbonization through electrification. Inspired by trends in the automotive industry, hybrid electric propulsion systems are increasingly being proposed and used on ships to achieve greater energy efficiency [4].

Currently, the majority of electric propulsion systems used in vessels are based on an alternating current (AC) distribution network. Despite their widespread use, they present significant drawbacks in their application, such as the need to synchronize generation units, manage reactive power flow, control transformer starting currents, handle harmonic currents, mitigate three-phase imbalances [5], and reduce system efficiency, as motors operate at a constant speed [6].

* Corresponding author.
E-mail addresses: dslozano@ujaen.es (D. Sánchez-Lozano), ramolina@ujaen.es (R. Aguado), aescamez@ujaen.es (A. Escámez), joseantonio.hernandez@dimme.uhu.es (J.A. Hernández-Torres), juan.perez@die.uhu.es (J.P. Torreglosa), dvera@ujaen.es (D. Vera).

https://doi.org/10.1016/j.enconman.2025.119859
Received 3 December 2024; Received in revised form 22 April 2025; Accepted 24 April 2025
Available online 21 May 2025

Nomenclature

Symbols

$\dot{m}$	Mass flow rate [kg s^{-1}]
$\dot{Q}$	Heat flow rate [kW]
$\dot{W}$	Power [kW]
η	Efficiency
c_p	Mass heat capacity at constant pressure [kJ kg^{-1} K^{-1}]
H	Enthalpy [kJ]
h	Mass enthalpy [kJ kg^{-1}]
n	Life span
P	Power [kW]
p	Pressure [bar]
S	Entropy [kJ K^{-1}]
s	Mass entropy [kJ $kg^{-1}K^{-1}$]
T	Temperature [°C]
t	Time period
U	Global heat transfer coefficient [W m^{-2} K^{-1}]
V	Voltage [V]

Subscripts

a	Ambient
$bottom$	Bottoming power cycle
$cond$	Condenser
$conv$	Power conversion
e	Electrical
eg	Exhaust gas
em	Electromechanical
$evap$	Evaporator
exp	Expander
f	Feedstock or fuel
gen	Generator
$gross$	Gross electricity
htf	Heat transfer fluid
hx	Heat exchanger
i	Isentropic
ip	inner pipe
k	Component
l	loss
lm	logarithmic mean
m	Mechanical
net	Net electricity
og	Off-gas
op	outer pipe
$pump$	Pump
reg	Regenerator
sw	Sea water
wf	Working fluid

Abbreviations

TIT	Turbine inlet temperature
AC	Alternating current
CEPCI	Chemical Engineering Plant Cost Index
CHP	Combined heat and power
DC	Direct current
DFCI	Direct fixed-capital investment
DG	Diesel generator
DPB	Discounted payback
EG	Exhaust gas
FCI	Fixed-capital investment
GWP	Global warming potential
HRSG	Heat recovery steam generator
HSW	Hot sanitary water
HT	High temperature
HTF	Heat transfer fluid
HTHX	High-temperature heat exchanger
HTS	High-temperature source
HX	Heat exchanger
IFCI	Indirect fixed-capital investment
INV	Investment
IRR	Internal rate of return
LT	Low temperature
NCF	Net cash flow
NPFA	National Fire Protection Association
NPV	Net present value
O&M	Operational and maintenance
ODP	Ozone depletion potential
ORC	Organic Rankine cycle
PEC	Purchase equipment cost
PI	Profitability index
SFOC	Specific fuel oil consumption
WACC	Weighted average cost of capital
WF	Working fluid
WHR	Waste-heat recovery

Due to these challenges and the recent advancements in the field of semiconductors [7], a transformation is underway in the maritime sector through the implementation of direct current (DC) distribution systems. In DC distribution, the mechanical energy generated by diesel engines is converted into electricity in AC through synchronous generators. AC is converted to DC through rectifiers connected to the DC distribution network. For propulsion, the propellers are connected to the DC network through sets of inverter controllers and induction machines [8]. For the connection of AC loads, inverters are used, which may be connected to transformers to adjust the output voltage, if necessary.

A DC distribution system offers several advantages. Firstly, it reduces the number of conversion stages, simplifying the system architecture [8]. Secondly, it enables weight reduction and a more flexible equipment arrangement [5]. Additionally, synchronization units are unnecessary, streamlining design and operation [9]. Furthermore, it enhances energy efficiency by optimizing generation system operation, leading to reduced fuel consumption and emissions. Moreover, the system minimizes noise and decreases mechanical and thermal loads on the engine [10]. It also facilitates the integration of renewable energies and the implementation of storage systems [5]. Lastly, its robustness against failures is ensured by power electronics, allowing immediate control of the electrical variables to prevent failures from spreading through the network and disturbing voltage and frequency [10].

The main sources of thermal energy that can be harnessed in ships include the exhaust gases generated by the engines and cooling flows [11]. Indeed, a substantial fraction, around 50%, of the total thermal energy contained in the fuel is dissipated as heat [12]. It is noteworthy that about 26% of this thermal energy is contained in the exhaust gases [12].

Organic Rankine cycles (ORC) are innovative systems that utilize organic fluids to achieve higher efficiencies in recovering heat at temperatures below 400 °C [13]. Most studies on ORC systems have largely focused on industrial applications [14], with limited exploration of their use in maritime settings. Ongoing research is now focused on the application of ORC units for recovering waste heat in ships, where its potential to reduce fuel consumption and CO_2 emissions in maritime transport is significant, driven by the need to adapt ships to new regulations. Recent publications have assessed the feasibility of ORC units for recovering residual heat in marine diesel engines. These systems are promising alternatives for efficiently recovering heat at lower temperatures, and active efforts are currently underway to optimize this technology for implementation in the maritime sector [12,14–18]. For example, Konur et al. [19] analyzed an ORC system for recovering waste heat from exhaust gases in the marine diesel generators of an oil/chemical tanker. The system was thermodynamically modeled, resulting in the optimization of the organic fluid, with R1336mzz(Z) being selected. This optimization led to a 15% reduction in fuel usage, resulting in an annual reduction of emissions totaling 849.63 t CO_2, 6.96 t SO_X, and 24.79 t NO_X. In addition, Yang et al. [20] evaluated a waste heat recovery (WHR) system applying an ORC system with R245fa as organic working fluid, achieving annual savings of 489,000 kg of diesel fuel, resulting in a 76% reduction in CO_2 emissions per kWh generated compared to the conventional diesel scenario. Pallis et al. [21] utilized jacket cooling water to design and manufacture a small-scale prototype of a marine ORC heat recovery system. R134a was chosen as the working fluid, with 2500 kW_{th} available from the cooling water, resulting in a net electric power of 170 kW_e. With this electrical power output, a total electricity generation of 1145 MWh_e can be produced annually if the system operates continuously. Zeng et al. [22] devised an ORC system to harness all the available heat sources from a ship, including exhaust gases, scavenged air, and jacket cooling water waste heat. R245fa was used as the working fluid. Their findings revealed that this technology allowed for an increase in the net output power of the system from 431 W to 526 W. Finally, ChunWee et al. [23] addressed the implementation of ORC units in marine vessels for WHR, focusing on an offshore service vessel. The economic analysis indicated a potential annual fuel savings of 5 to 9%, with a specific installation cost of $5000-8000 $/kW. The ORC in a simple cycle configuration with methanol as the working fluid exhibited the shortest payback period. Additionally, an entropy generation analysis was conducted, emphasizing the importance of improving heat exchangers to reduce entropy generation.

The main novelty of the proposed approach lies in the detailed simulation, off-design optimization, and techno-economic assessment of an ORC unit tailored for marine diesel-electric propulsion, utilizing advanced DC distribution networks. By harnessing the thermal energy available in the exhaust gas from diesel generators, this study demonstrates significant potential for reducing fuel consumption and emissions, thereby contributing to the decarbonization goals of the maritime sector. This work incorporates off-design optimization, an essential yet underutilized technique, to assess the ORC system's performance under varying load conditions on actual ship routes. Additionally, very few studies in the scientific literature have conducted comprehensive techno-economic assessments of onboard ORC systems. This research provides a comparative analysis that considers both technical performance and economic viability, including a detailed sensitivity analysis, which is essential for practical implementation. Moreover, economic and emissions analysis is based on real ship routes, a perspective that has been largely overlooked in the literature. Lastly, the integration of ORC units in modern DC distribution networks on ships remains highly underexplored in scientific research. This paper addresses this gap, demonstrating the benefits of using DC systems to improve energy efficiency and reduce greenhouse gas emissions.

The remainder of this article is structured as follows. Section 2 introduces the case study on the application of ORC systems in diesel-electric propulsion in ships, as well as a description of the software used to simulate the integrated ORC system, the underlying assumptions of the model, and the calculation methods. Section 3 provides an in-depth performance analysis of the ORC system, including a screening and comparison of various working fluids, their efficiencies, and thermodynamic behavior under different operating conditions, as well as a comprehensive evaluation using an elaborately designed Sankey diagram to illustrate energy flows and system efficiency. This section also investigates the off-design performance of the ORC system and its performance under typical conditions, in addition to an assessment of the energy efficiency of a cruise ship's actual route, including the effect of integrating an ORC system on fuel consumption and emissions. An extensive economic feasibility assessment of the proposed ORC system, including a detailed sensitivity analysis, is also provided at the end of this section. Finally, a few concluding remarks are presented in Section 4.

2. Methods

In this section, the case study is first introduced, providing the context and operating conditions under which the ORC system is evaluated. Subsequently, the procedure for selecting the most suitable organic and heat transfer fluids is described, considering their thermodynamic properties, environmental impact, and compatibility within the simulation framework. Afterwards, the mathematical model used for system analysis is presented, incorporating key aspects such as heat transfer efficiency and design parameters. Finally, the approach for the economic study is outlined, detailing the financial formulas and the framework to assess the economic feasibility of the system.

In this case study, the integration of an ORC unit into the marine diesel propulsion system of a shuttle tanker is investigated. The main goal is to explore the potential benefits of utilizing waste heat recovery through ORC technology to enhance energy efficiency and reduce fuel consumption in marine applications. The selected case study vessel is a single-screw shuttle tanker, which is equipped with dual diesel generators that provide the necessary power for propulsion in a DC distribution system.

For simulation and optimization of the ORC system for marine diesel DC propulsion systems, the simplified model shown in Fig. 1 is used, based on the electrical layout of a single-screw shuttle tanker with propulsion [24], commonly used on real ships. The model consists of two zones. Each zone represents the installation of two energy systems composed of two diesel generators, specifically using the 12V46F model from the manufacturer Wärtsilä (Finland), which delivers a full load electrical power of 14.4 MW (18 MVA). In practice, one of the generation systems is installed on the port side and the other on the starboard side [25], with two diesel generators in each zone. This results in a net energy generation at full load of 57.6 MW (72 MVA). The scheme is complemented by the inclusion of rectifiers to convert the AC power from the diesel generator into DC power, as well as inverters to supply the propulsion system with AC.

The simulation of diesel generators is the starting point of this study. The technical features of the 12V46F marine diesel generator manufactured by Wärtsilä are reported in Table 1.

The integrated ORC system proposed in the study, shown in Fig. 2, consists of two ORC units placed on the bow and the starboard. Consequently, the study only considers two of the four available diesel generators. For hot sanitary water (HSW) production, the same engine cooling water circuit is utilized. Regarding the ORC system, it comprises a mixer where the two exhaust gas pipes from the diesel generators are combined. The combined exhaust gas flows through a high-temperature heat exchanger (HTHX) where the gases transfer heat to a heat transfer fluid loop, recommended to prevent potential local overheating and chemical instability of the organic fluid. Subsequently, in an evaporator, the organic working fluid (WF) is heated before passing through the expander to generate electrical energy. As the WF exits the expander, it passes through a regenerator designed to

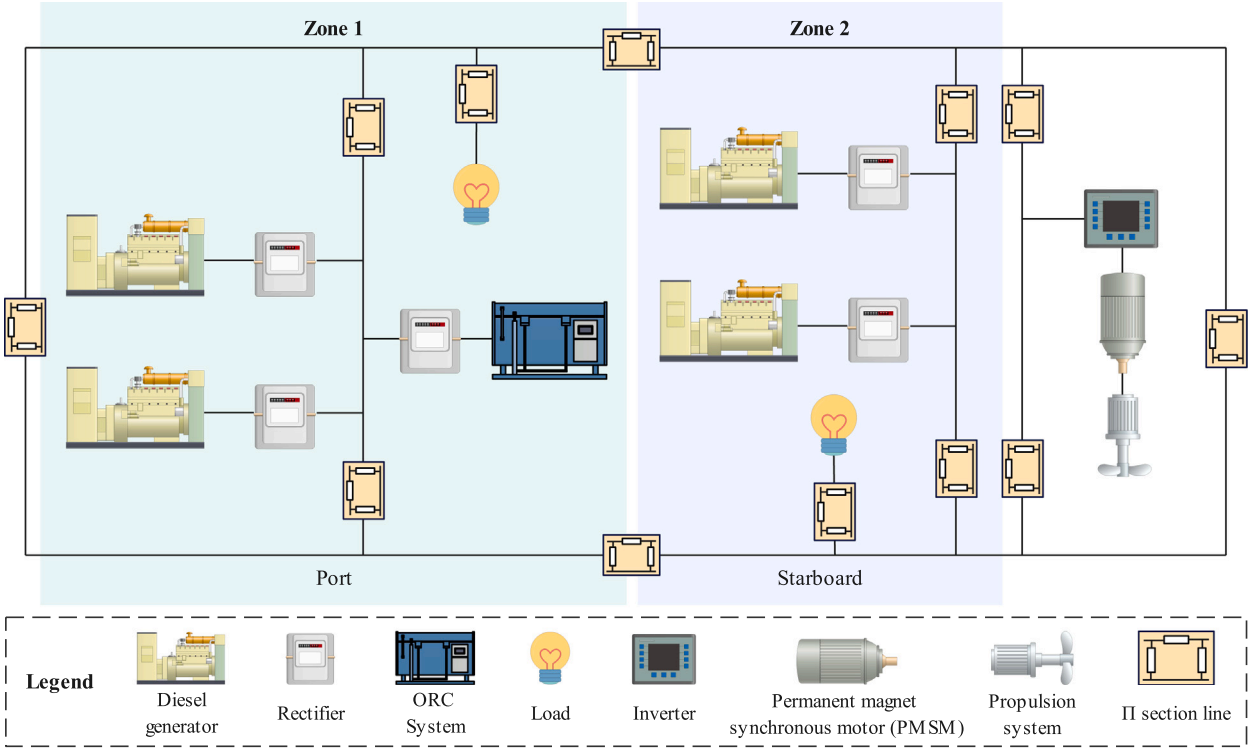

Fig. 1. Schematic diagram of the DC propulsion vessel selected for the application of the ORC system.

Table 1
Representative characteristics of Wärtsilä 12V46F diesel generator for offshore applications [26].

Parameter		Value	Unit
Electrical power output (AC)		14.4	MW_e
Angular speed		600	rpm
Combustion air flow at 100% load		25.1	kg/s
Temperature after air cooler		50	°C
Exhaust gas system	Flow at 100% load	25.95	kg/s
	Flow at 85% load	22.44	kg/s
	Flow at 75% load	21.84	kg/s
	Flow at 50% load	17.40	kg/s
	Exhaust temperature 100% load	364	°C
	Exhaust temperature 85% load	330	°C
	Exhaust temperature 75% load	330	°C
	Exhaust temperature 50% load	297	°C
Fuel system	SFOC at 100% load	182.5	g/kWh_e
	SFOC at 85% load	176.8	g/kWh_e
	SFOC at 75% load	185.9	g/kWh_e
	SFOC at 50% load	195	g/kWh_e
Cooling water system	Water temperature inlet	74	°C
	Water temperature outlet	91–95	°C

extract some of the available heat from the WF and transfer it back to the previous stage before entering the evaporator. Finally, the WF passes through a condenser that utilizes seawater, further reducing its temperature before being introduced to the pump to increase its pressure for continuous repetition of the cycle.

2.1. Selection of the organic working fluid and the heat transfer fluid

Selecting a suitable organic fluid is a critical aspect in the design and modeling of an ORC system [27–30]. The choice of one working fluid over another significantly impacts cycle performance and efficiency [27,29–31], as well as thermodynamic and plant design parameters and applicable safety requirements [27].

The selection of the appropriate working fluid largely depends on two main characteristics: the heat source temperature [27,30] and the ORC configuration [30,31]. For these reasons, it is important for the fluid to have suitable critical constants, low molecular complexity, and a boiling point compatible with the condenser [27]. Additionally, other important aspects such as availability, price, flammability, toxicity, chemical stability [27], and environmental impact [27,30,32] should be taken into account, as well as safety considerations during handling and operation [32]. Regarding environmental aspects, Table 2 highlights indicators such as ozone depletion potential (ODP), global warming potential over a 100-year period (GWP_{100}) [27,28,30,31,33], as well as the NPFA 704 standard for material hazard identification by the National Fire Protection Association (NPFA), which provides information on health risks (H), fire hazard (F), and instability (I) on a scale from 0 (low hazard) to 4 (very hazardous) [34]. EU guidelines and the Montreal Protocol report criteria for WF selection, including a maximum GWP of 150 and zero ODP, while also considering the NPFA 704 hazard rating [35]. In the working fluid selection process, it is

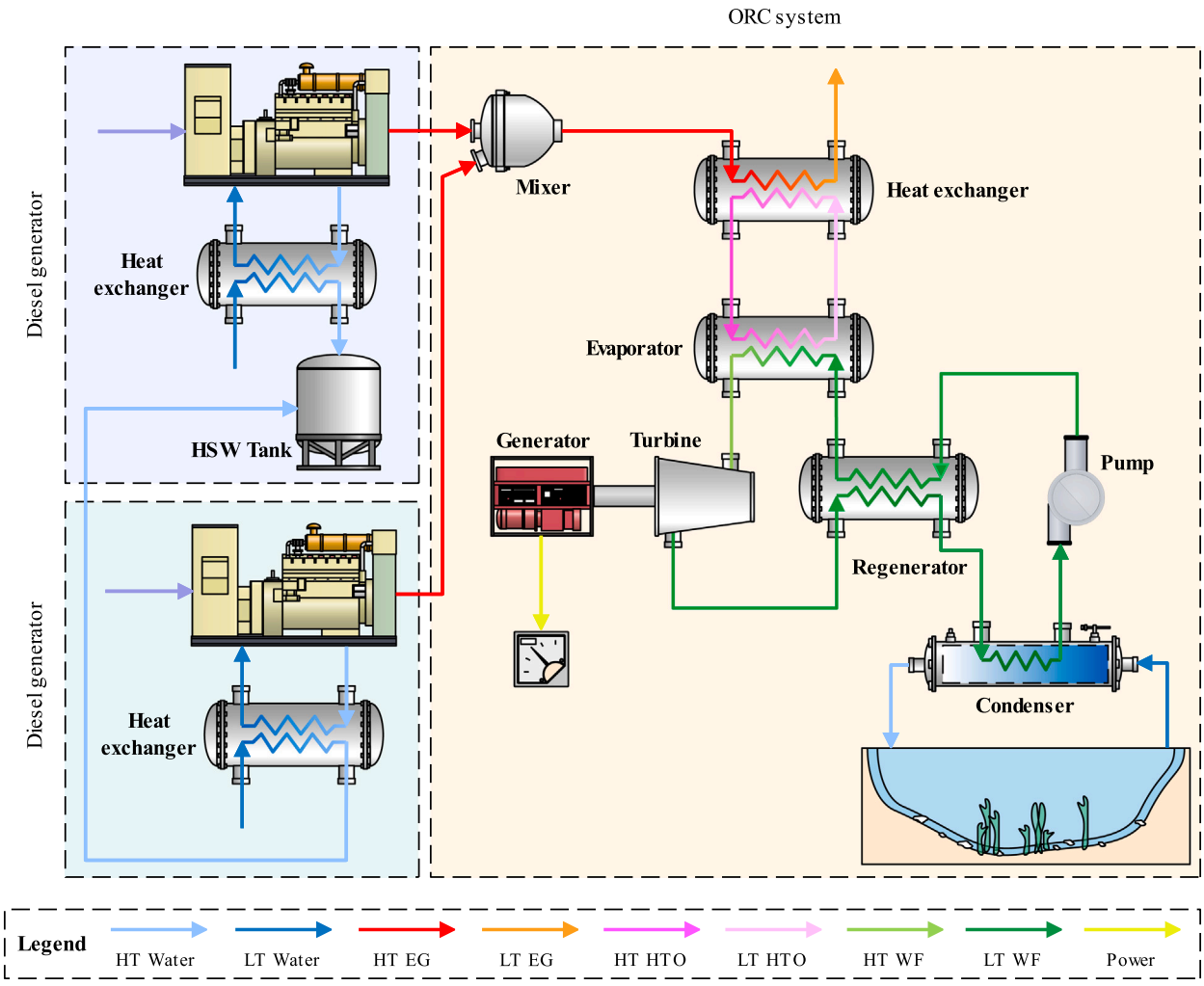

Fig. 2. Schematic diagram of the integrated ORC.

advisable that the condenser pressure be as close to atmospheric pressure as possible [28], thus avoiding problems derived from operation, maintenance, and costs of a vacuum condenser. For successful selection of organic fluid, a trade-off among all selection criteria is necessary, as there is likely no fluid that is suitable in all the aspects discussed earlier [27,28].

Numerous organic working fluids have been suggested in the scientific literature for ORC systems driven by high-temperature sources (HTS) [30]. These organic working fluids include toluene (T_{cond} = 319 °C), ethylbenzene (T_{cond} = 344 °C), decane (T_{cond} = 345 °C), and cyclohexane (T_{cond} = 281 °C) [30,36,37], cyclopentane (T_{cond} = 239 °C), cyclohexane (T_{cond} = 280 °C), and benzene (T_{cond} = 289 °C) [33]. Temperatures ranging from 250–350 °C are applicable for HTS ORC cycles [33]. Accordingly, the exhaust gas temperatures between 330–350 °C of the present study are suitable for these ORC systems.

Table 2 reports the thermodynamic and environmental properties of the working fluids that meet the requirements for application to the ORC system under study, which is driven by an HTS between 250–350 °C. All of these properties were retrieved from the RefProp database.

In addition to the organic working fluid, it is highly recommended to include an additional heat transfer circuit to prevent potential local overheating and chemical instability of the organic working fluids [30]. Accordingly, a highly stable silicone heat transfer fluid composed of dimethyl polysiloxane was selected. It has a long lifespan and low fouling potential and is designed to operate in the liquid phase within the temperature range of −40 to 398.9 °C. The heat transfer fluid is designed to operate at a temperature of 340 °C.

2.2. Simulation of the integrated organic Rankine cycle unit

Thermoflex®, a product developed by Thermoflow Inc. (Jacksonville, FL, USA), was used as the simulation software [38]. This program provides simulation and modeling tools for various types of power plants, ranging from combined cycles and conventional steam cycles to repowering projects, in addition to a wide variety of renewable energy systems [45–48]. The standout feature that led to its selection is its extensive library of commercial products, including engine–generator sets that can be easily customized to fit any other engine from selected manufacturers. Fig. 3 illustrates the schematic used for modeling the diesel generators and generating HSW, as well as for simulating the ORC unit. The system comprises two fundamental modeling blocks: the diesel generators and the ORC system. Below are detailed descriptions of the specific features of each of these subsystems along with their respective modeling approaches.

- For simulation of diesel generators, the manufacturer's parameters provided in the technical manual for the Wärtsilä 12V46F diesel generator shall be followed [26]. The key technical specifications of these engine–generator sets are summarized in Table 1.
- The ambient air temperature is assumed to be 15 °C.
- Kim et al. [49] reported a seawater temperature of 20 °C for its condenser, while Sellers et al. [12] considered a higher temperature, specifically 29 °C. Another study by Chen et al. [50]

Table 2
Thermodynamic properties of typical organic working fluids proposed for waste heat recovery from high temperature sources [27,28,32,33,38–41].

Organic fluid	Molar mass	Critical temperature	Critical pressure	Condensation temperature	Condensation pressure	Degradation temperature	Environmental issues[b]				
	kg/kmol	°C	bar	°C @ 1 bar	bar @ 45 °C	°C	GWP_{100}[a]	ODP	H	F	I
Cyclopentane	70.13	239	45.83	48.85	0.880	260–280 [42]	4–6	0	1	3	0
Cyclohexane	84.16	280	40.80	80.28	0.300	N/A	4–6	0	1	3	0
Benzene	78.11	289	49.07	79.64	0.299	315 [42]	3–4	0	2	3	0
Toluene	92.14	319	41.26	110.00	0.099	315 [42]	3–4	0	2	3	0
Acetone	58.08	235	46.92	55.69	0.684	>462 [43,44]	0.5	0	1	3	0
DMC	90.08	284	49.09	89.69	0.188	N/A	3–4	0	3	3	0
Heptane	100.21	267	27.36	97.95	0.154	260 [42]	3	0	1	3	0
Methylcyclohexane	98.19	299	34.70	100.00	0.151	N/A	2.7	0	1	3	0
Hexane	86.18	235	30.44	68.30	0.451	260–280 [42]	3	0	1	3	0

[a] GWP_{100}: Global warming potential in a 100-year period.
[b] Safety information according to the hazard rating system by the National Fire Protection Association (NPFA) of the United States. Each of the health (H), flammability (F) and instability (I) hazards is rated on a scale from 0 (no hazard) to 4 (severe hazard).

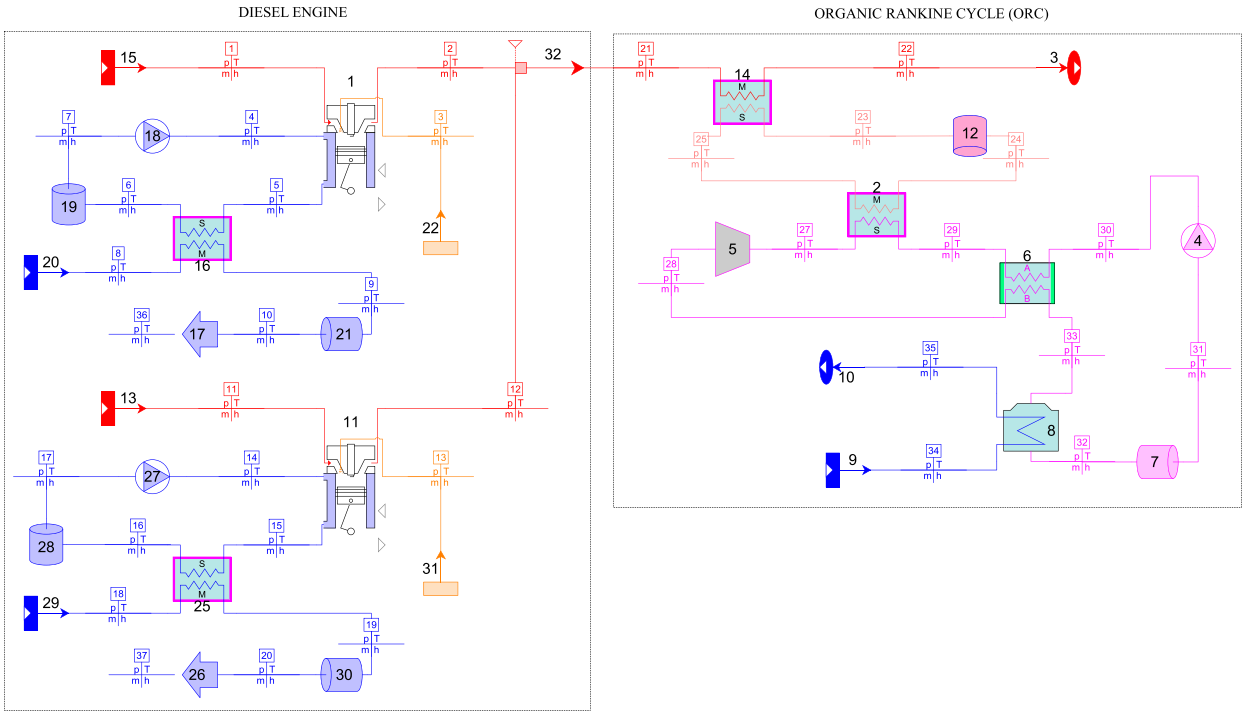

Fig. 3. Process simulation flowsheet of the integrated ORC system in Thermoflex.

suggested that the temperature throughout the year varies between the two previously mentioned values. Kosmadakis and Neofytou [51] assumed that the condenser heat is rejected to a central freshwater cooler with the cooling water entering at a temperature of 25 °C. Similarly, Lion et al. [52] considered a temperature of 25 °C, which is an average temperature and is selected for the simulation.

- The system is evaluated for a turbine inlet pressure of 20 bar [27,28,30]. In the model, the turbine inlet temperature (TIT) leading to the highest net electrical efficiency is selected for each of the evaluated organic fluids.
- The minimum temperature of the off-gas exiting the HTHX, which transfers heat to the HTF circuit supplying the evaporator of the ORC unit, is set at 120 °C [39].

Table 3 presents the operating parameters used in the design of the ORC equipment, as well as the assumptions adopted in the heat exchanger equipment for HSW production.

Since the overall heat-transfer coefficient for each component in Table 3 is known, the heat transfer area of each heat exchanger can be calculated using Eq. (1) [39], which is valid for counter-current flows.

$$\dot{Q} = U\ A\ \Delta T_{lm} \tag{1}$$

where ΔT_{lm} is the logarithmic average temperature difference for each component. This parameter is determined as follows:

$$\Delta T_{lm} = \frac{(T_{op,in} - T_{ip,out}) - (T_{op,out} - T_{ip,in})}{\ln\left(\frac{T_{op,in} - T_{ip,out}}{T_{op,out} - T_{ip,in}}\right)}. \tag{2}$$

where op and ip refer to the outer and the inner pipe, respectively [39].

Table 4 provides a summary of the mass and energy balances for key components of the ORC system, together with their corresponding energy efficiencies. Note that $\dot{Q}_l$ represents the heat flow loss associated with each individual component, indicating the energy lost through heat transfer. The numbers used for the identification of the different equipment and flow rates are based on the process simulation flowsheet of the integrated ORC system in Thermoflex, previously shown in Fig. 3.

The following equation is used to calculate the thermodynamic efficiency of the ORC:

$$\eta_{ORC} = \frac{\dot{W}_{exp} - \dot{W}_{pump}}{\dot{m}_{wf}\ \Delta h_{evap}} \tag{3}$$

Table 3
Design parameters of the ORC bottoming power unit.

Equipment	Performance parameter	Value	Unit	Reference(s)
Expander	Inlet pressure	20	bar	[27,28]
	Isentropic efficiency	85	%	[27,53–56]
	Mechanical efficiency	97	%	[27]
High-temperature heat exchanger	Heat transfer efficiency	90	%	[30]
	Minimum pinch point	10	°C	[27,57]
	Pressure drop	5	%	[53]
	Global heat transfer coefficient	502	W/m^{2}K	[58]
Evaporator	Heat transfer efficiency	90	%	[59]
	Minimum pinch point	10	°C	[27,30,57]
	Pressure drop	5	%	[53]
	Global heat transfer coefficient	539	W/m^{2}K	[58]
Regenerator	Heat transfer efficiency	90	%	[30]
	Minimum pinch point	10	°C	[27,30,57]
	Pressure drop	5	%	[53]
	Global heat transfer coefficient	1059	W/m^{2}K	[58]
Condenser	Condenser pressure	0.1–1	bar	[27,28,30]
	Heat transfer efficiency	95	%	Estimated
	Minimum pinch point	10	°C	[27,57]
	Pressure drop	2	%	[14]
	Maximum temperature outlet	60	°C	[18]
	Global heat transfer coefficient	833	W/m^{2}K	[58]
Pump	Isentropic efficiency	80	%	[14,27,30]
	Mechanical efficiency	97	%	[27,54]
Hot sanitary water heat exchanger	Heat transfer efficiency	85	%	[30]
	Minimum pinch point	10	°C	[27,57]
	Pressure drop	5	%	[53]
Generator	Electrical efficiency	97	%	[28]

Table 4
Mass and energy balance analysis for each component of the ORC system.

N°	Component	Mass balance	Energy balance	Energy efficiency
1	Maritime DG	$\dot{m}_1 + \dot{m}_4 + \dot{m}_3 = \dot{m}_2 + \dot{m}_5$	$\dot{m}_1\, h_1 + \dot{m}_3\, h_3 + \dot{m}_4\, h_4 = +\dot{m}_2\, h_2 + \dot{m}_5\, h_5 + \dot{W}_{DG} + \dot{Q}_{l,DG}$	$\eta_{DG} = \frac{\dot{W}_{DG}}{\dot{m}_3\, PCI_f}$
16	HSW HX	$\dot{m}_2 + \dot{m}_5 = \dot{m}_6 + \dot{m}_9$	$\dot{m}_5\,(h_5 - h_6) = \dot{m}_8\,(h_9 - h_8) + \dot{Q}_{l,hsw,hx}$	$\eta_{hsw,hx} = \frac{\dot{m}_8\,(h_9 - h_8)}{\dot{m}_5\,(h_5 - h_6)}$
18	Water cooling pump	$\dot{m}_7 = \dot{m}_4$	$\dot{m}_7\, h_7 = \dot{m}_4\, h_4 + \dot{W}_{pump} + \dot{Q}_{l,pump}$	$\eta_{pump} = \frac{\dot{m}_4\, h_4}{\dot{m}_7\, h_7 + \dot{W}_{pump}}$
14	HTF HX	$\dot{m}_{21} + \dot{m}_{23} = \dot{m}_{22} + \dot{m}_{25}$	$\dot{m}_{21}\,(h_{21} - h_{22}) = \dot{m}_{23}\,(h_{25} - h_{23}) + \dot{Q}_{l,htf,hx}$	$\eta_{htf,hx} = \frac{\dot{m}_{23}\,(h_{25} - h_{23})}{\dot{m}_{21}\,(h_{21} - h_{22})}$
2	Evaporator	$\dot{m}_{25} + \dot{m}_{29} = \dot{m}_{27} + \dot{m}_{23}$	$\dot{m}_{25}\,(h_{25} - h_{23}) = \dot{m}_{29}\,(h_{27} - h_{29}) + \dot{Q}_{l,evap}$	$\eta_{evap} = \frac{\dot{m}_{29}\,(h_{27} - h_{29})}{\dot{m}_{25}\,(h_{25} - h_{23})}$
5	Expander	$\dot{m}_{27} = \dot{m}_{28}$	$\dot{m}_{27}\, h_{27} = \dot{m}_{28}\, h_{28} + \dot{W}_{exp} + \dot{Q}_{l,exp}$	$\eta_{exp} = \frac{\dot{W}_{exp}}{\dot{m}_{27}\,(h_{27} - h_{28})}$
6	Regenerator	$\dot{m}_{28} + \dot{m}_{30} = \dot{m}_{29} + \dot{m}_{33}$	$\dot{m}_{28}\,(h_{33} - h_{28}) = \dot{m}_{29}\,(h_{29} - h_{30}) + \dot{Q}_{l,reg}$	$\eta_{reg} = \frac{\dot{m}_{29}\,(h_{29} - h_{30})}{\dot{m}_{28}\,(h_{33} - h_{28})}$
8	Condenser	$\dot{m}_{33} + \dot{m}_{34} = \dot{m}_{32} + \dot{m}_{35}$	$\dot{m}_{34}\,(h_{35} - h_{34}) = \dot{m}_{33}\,(h_{33} - h_{32}) + \dot{Q}_{l,cond}$	$\eta_{cond} = \frac{\dot{m}_{33}\,(h_{33} - h_{32})}{\dot{m}_{34}\,(h_{35} - h_{34})}$
4	WF pump	$\dot{m}_{31} = \dot{m}_{30}$	$\dot{m}_{30}\, h_{30} = \dot{m}_{31}\, h_{31} + \dot{W}_{wf,pump} + \dot{Q}_{l,wf,pump}$	$\eta_{wf,pump} = \frac{\dot{m}_{30}\, h_{30}}{\dot{m}_{31}\, h_{31} + \dot{W}_{wf,pump}}$

where, η_{ORC} stands for the thermodynamic efficiency of the ORC, $\dot{W}_{exp}$ represents the output power of the expander, $\dot{W}_{pump}$ denotes the power consumed by the pump, $\dot{m}_{wf}$ indicates the mass flow rate of the working fluid (wf), and Δh_{evap} denotes the enthalpy change during the evaporation process. Accordingly, Eq. (3) quantifies the efficiency of heat conversion into useful work, considering both the power output at the expander and the power input required to drive the working fluid through the cycle.

The efficiency of the whole bottoming power unit, including the heat transfer fluid (HTF) circuit, is calculated as follows:

$$\eta_{\mathrm{htf}} = \frac{\dot{W}_{exp} - \dot{W}_{pump}}{\dot{m}_{htf}\,\Delta h_{htf,\mathrm{HTHX}}} \tag{4}$$

The net power output ($\dot{W}_{\mathrm{bottom}}$) available at the bottom of the ORC unit is obtained through the following expression:

$$\dot{W}_{bottom} = \eta_{gen}\,\dot{W}_{exp} - \eta_{em}\,\dot{W}_{pump} \tag{5}$$

where $\dot{W}_{exp}$ represents the power output of the system, adjusted by the power generation efficiency of the generator (η_{gen}). Moreover, $\dot{W}_{pump}$ denotes the power consumed by the pump, with (η_{em}) representing its electromechanical efficiency.

The efficiency of the bottoming power cycle (η_{bottom}) is calculated as follows:

$$\eta_{bottom} = \frac{\dot{W}_{bottom}}{\dot{m}_{eg}\, c_{p,eg}\,(T_{eg} - T_a)} \tag{6}$$

Table 5
Purchase cost correlations of the ORC equipment. All costs are expressed in US dollars.

Equipment	Cost correlation	CEPCI		Sources
		Year	Value	
Condenser	$C_{cond} = 516.62 \times (A_{cond})^{0.85}$	2000	394.1	[57,60–63]
Evaporator	$C_{evap} = 309.14 \times (A_{evap})^{0.85}$	1997	386.5	[57,60,61,63]
HTF heat exhanger	$C_{HX,htf} = 309.14 \times (A_{HX,htf})^{0.85}$	1997	386.5	[57,60,61,63]
Regenerator	$C_{reg} = 309.14 \times (A_{reg})^{0.85}$	1997	386.5	[57,60,61,63]
Expander	$C_{exp} = 4750 \times (\dot{W}_{exp})^{0.75}$	2010	550.8	[57,60–63]
Generator	$C_{gen} = 60 \times (\dot{W}_{gen})^{0.95}$	2001	394.3	[60,63]
Pump	$C_{pump} = 3540 \times (\dot{W}_{pump})^{0.71}$	2011	585.7	[63–65]

where $\dot{W}_{bottom}$ refers to the net power output of the ORC unit, $\dot{m}_{eg}$ denotes the mass flow rate of the exhaust gas, $c_{p,eg}$ represents the specific heat capacity of the exhaust gas, T_{eg} indicates the temperature of the exhaust gas and T_a represents the ambient temperature.

2.3. Economic feasibility assessment

This section presents the procedure for evaluating the economic performance of the ORC system. The capital cost of the ORC unit includes the purchase equipment cost (PEC) along with additional direct fixed-capital investments, indirect fixed-capital investments (IFCI), and other outlays. A detailed breakdown of these costs can be found in Section 3.5.

The PEC of the ORC unit was determined by aggregating the costs of its individual components using the empirical correlations provided in Table 5. The PEC of each heat exchanger in the bottoming power unit was calculated based on the required heat transfer area (A). Similarly, the PECs of the expander, generator, and pump were estimated based on their respective power ratings.

The economic data presented in Table 5 only reflect the value of the current year. The cost of each component is adjusted from the reference year to the current year (2024) using the Chemical Engineering Plant Cost Index (CEPCI) according to Eq. (7) [60–63].

$$C_{k,\text{present}} = C_{k,\text{reference}} \times \frac{\text{CEPCI}_{\text{present}}}{\text{CEPCI}_{\text{reference}}} \tag{7}$$

where $C_{k,\text{present}}$ represents the cost of the component k in the current year, $C_{k,\text{reference}}$ represents the cost of component k in the reference year, $\text{CEPCI}_{\text{present}}$ is the Chemical Engineering Plant Cost Index for the present year, and $\text{CEPCI}_{\text{reference}}$ is the Chemical Engineering Plant Cost Index for the reference year.

The economic feasibility assessment of the ORC system was conducted using standard financial appraisal methods. These include the net present value, internal rate of return, profitability index, and discounted payback period.

The net present value (NPV) represents the difference between the present value of the project's future cash flows and the initial investment [66,67]. This parameter reflects the earnings after recovering the initial capital investment (INV). Consequently, if NPV > 0, the project is profitable, while if NPV < 0, it results in a loss.

$$\text{NPV} = \sum_{t=1}^{n} \frac{\text{NCF}_t}{(1+\text{WACC})^t} - \text{INV} \tag{8}$$

where NCF_t is the net cash flow during period t, WACC is the weighted average capital cost used as the discount rate, INV is the initial capital investment, and n represents the project lifetime in years.

The time required to recover the initial investment, accounting for the annual discount rate, is known as the discounted payback period (DPB). This metric is calculated using Eq. (9), which assumes equal cash flows, making it applicable only for scenarios with constant cash inflows. Therefore, an average annual cash flow is used in this calculation.

$$\text{DPB} = \frac{\log\left(\dfrac{1}{1 - \dfrac{\text{INV} \times \text{WACC}}{\frac{\sum_{t=1}^{n} \text{NCF}_t}{n}}}\right)}{\log(1+\text{WACC})} \tag{9}$$

The internal rate of return (IRR) refers to the discount rate that results in a zero NPV for the project, indicating the maximum discount rate for which the investment breaks even.

$$\text{NPV} = \sum_{t=1}^{n} \frac{\text{NCF}_t}{(1+\text{IRR})^t} - \text{INV} = 0 \tag{10}$$

Finally, the profitability index (PI) is defined as the ratio of the net present value to the initial investment [67]. A PI value greater than unity indicates that the project is profitable.

$$\text{PI} = \frac{\text{NPV}}{\text{INV}} \tag{11}$$

3. Results and discussion

This section presents a detailed analysis of the integrated system's performance, including a comparison of various organic working fluids in terms of efficiency and thermodynamic behavior. A Sankey diagram is used to illustrate energy flows, losses, and efficiencies. Additionally, an off-design analysis is conducted to evaluate system performance under real operating conditions. Finally, an economic assessment is carried out to determine the system's feasibility and cost-effectiveness.

3.1. Integrated organic Rankine cycle and selection of the working fluid

Fig. 4 compares the bottoming efficiency (η_{bottom}) and the condensation temperature (T_{cond}) of the ORC unit for various organic working fluids as functions of the condenser pressure. The fluids examined include cyclopentane, cyclohexane, benzene, toluene, acetone, dimethyl carbonate (DMC), heptane, methylcyclohexane, and hexane. Each plot shows multiple curves corresponding to different turbine inlet temperatures (TIT). In particular, acetone and cyclopentane demonstrate the capability to achieve the lowest condensation temperatures without significant penalties in efficiency, even at higher condenser pressures. Under ambient pressure conditions for operating the condenser, the bottoming efficiency with these working fluids is in the range of 9%–10%. This makes them particularly advantageous because of their ability to operate the condenser at near ambient pressure to avoid air leakage, which may adversely affect the ORC unit if the condenser pressure is excessively low. Accordingly, trade-offs must be carefully considered when selecting a working fluid for specific

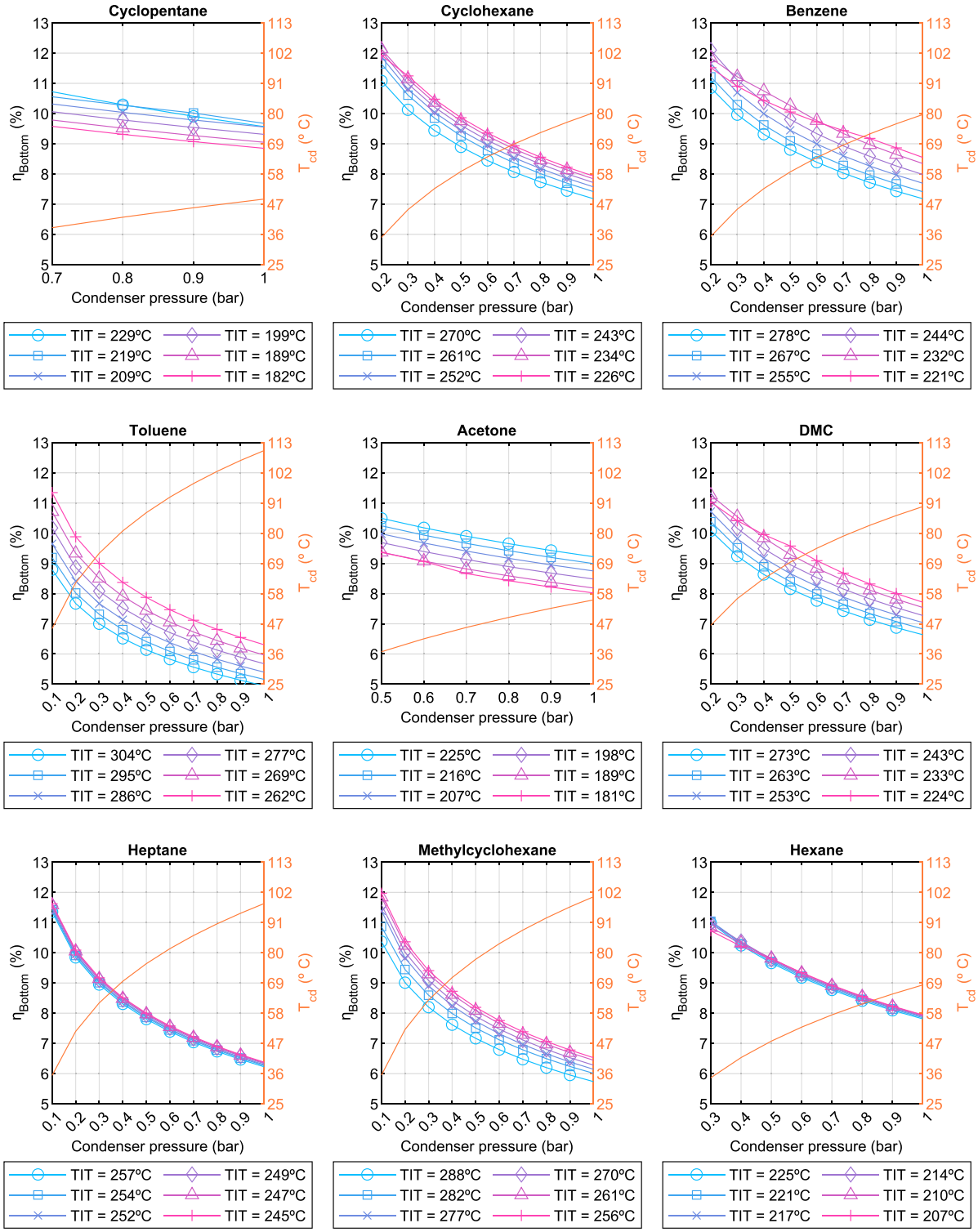

Fig. 4. ORC system performances for the different organic liquids tested at different condensation pressures.

thermodynamic cycles. Although other fluids may reach higher efficiencies under low-pressure conditions, they also suffer more pronounced efficiency reductions with increasing condenser pressure and exhibit higher minimum condensation temperatures. Benzene, for example, can achieve a comparable bottoming efficiency under ambient pressure, but its condensation temperature is significantly higher at 79.6 °C, compared to cyclopentane (48.8 °C) and acetone (55.7 °C).

Table 6 presents a comparative analysis of the efficiencies of the ORC using cyclopentane and acetone as working fluids under different engine load conditions (85% and 100%). The results indicate that the thermodynamic efficiency (η_{ORC}) is slightly higher for cyclopentane, with values of 20.02% and 20.30% for 85% and 100% engine load, respectively, compared to acetone, which has values of 18.73% and 19.09% under the same conditions. Similarly, the efficiency at the

Table 6
Performance parameters of the organic Rankine cycle under design conditions for the working fluids selected.

Performance parameter	Organic working fluid				Unit
	Cyclopentane		Acetone		
	85% engine load	100% engine load	85% engine load	100% engine load	
Exhaust gas temperature (T_{eg})	330	364	330	364	°C
Exhaust gas flow rate ($\dot{m}_{eg}$)	44.88	51.90	44.88	51.90	°C
Turbine inlet temperature (TIT)	214	220	218	225	°C
Condensation temperature (T_{cond})	48.85	48.85	55.69	55.69	°C
Condensation pressure (p_{cond})	1	1	1	1	bar
Pressure in evaporator (p_{evap})	20	20	20	20	bar
Off-gas temperature (T_{og})	120	123.6	120	120	°C
HTF mass flow rate ($\dot{m}_{htf}$)	22.09	25.89	22.22	24.88	kg/s
WF mass flow rate ($\dot{m}_{wf}$)	15.41	20.33	12.41	16.63	kg/s
Sea water mass flow rate ($\dot{m}_{sw}$)	102.7	188.4	70.97	95.05	kg/s
UA HTF HX	895.2	1028.9	894.3	705.2	kW/°C
UA evaporator	414.1	404.6	288.5	500.1	kW/°C
UA regenerator	112.3	112.3	63.3	63.3	kW/°C
UA condenser	364.7	536	325.5	435.9	kW/°C
Pump power consumption ($\dot{W}_{pump}$)	89.08	117.7	68.67	92.0	kW
Gross electric power ($\dot{W}_{bottom,gross}$)	1813.48	2322.10	1598.17	2195.43	kW
Net electric power ($\dot{W}_{bottom,net}$)	1724.40	2204.40	1529.5	2103.43	kW
Thermodynamic efficiency (η_{ORC})	20.02	20.30	18.73	19.09	%
HTF efficiency (η_{htf})	18.02	18.27	16.85	17.18	%
Net electrical efficiency (η_{bottom})	9.04	9.65	8.45	9.20	%

HTHX (η_{htf}) follows the same trend, with cyclopentane showing values of 18.02% and 18.27%, whereas acetone achieves 16.85% and 17.18% for the respective engine loads.

Regarding the net electrical efficiency (η_{bottom}), cyclopentane again demonstrates a slight advantage over acetone. For an engine load of 85%, cyclopentane achieves an efficiency of 9.04%, and for a 100% load, it reaches 9.65%. In comparison, acetone has efficiencies of 8.45% and 9.20% under the same conditions. These findings suggest that cyclopentane is a marginally more efficient working fluid than acetone in terms of converting thermal energy to electrical energy, potentially making it a better choice for specific applications in ORC units under the evaluated operating conditions.

The temperature–specific entropy (T–s) diagram of the two analyzed fluids for the offshore diesel generators operating at 100% load is presented in Fig. 5. The T–s diagram of the ORC with cyclopentane as WF illustrates the operation between temperatures of 45 °C and 220 °C, while the T–s diagram of acetone operates at a higher TIT of 225 °C. In both cycles, the first stage is compression, where the pressure of the working fluid (WF) increases, causing a slight rise in temperature. The WF then undergoes heating and evaporation. During this stage, its temperature increases in the regenerator, and it evaporates by transferring heat from a high-temperature heat transfer fluid (HTF), which significantly raises its entropy. When the working fluid reaches the desired turbine inlet temperature (TIT), it expands in the turbine, doing useful work and further increasing its entropy. After leaving the expander, the WF passes through the regenerator to recover some residual heat. Finally, in the condensation stage, the WF releases heat to the cooling water (CW) and condenses at 45 °C. It is noteworthy that assuming a condensation temperature of 45 °C is a rather conservative approach, as it provides a safety margin that ensures a minimum pinch point temperature difference of at least 10 °C if the surface seawater temperature is close to 30 °C.

Despite its slightly lower efficiency, acetone is preferable to cyclopentane due to its lower cost and global warming potential, with similar safety aspects to those of cyclopentane, as outlined in Table 2. Pantaleo et al. [39] compared the performance of ORC power units in waste-heat recovery (WHR) applications for a broad range of working fluids. Their findings revealed that acetone consistently yielded the highest optimized power output, with the exception of the single-stage screw expander, where cyclopentane performed comparably. Additionally, the study assessed exergy losses, determining that the optimal fluid minimizes exergy losses in both the condenser and evaporator. Acetone was again the best option, as it resulted in the lowest overall exergy losses in the heat exchangers.

To further validate the decision to select acetone as the working fluid, the associated exposure risks in maritime environments were assessed. Acetone is preferred over cyclopentane due to its higher water solubility, which facilitates rapid dilution and mitigates the risks associated with surface contamination and bioaccumulation [68]. Moreover, acetone is readily biodegradable by microorganisms in both soil and aquatic environments, further supporting its environmental compatibility [68]. By contrast, cyclopentane is largely insoluble in water [69], leading to the formation of persistent surface layers that can detrimentally affect marine ecosystems. Cyclopentane is toxic to aquatic organisms, and it is strongly advised not to let the chemical enter the marine environment [70].

On the other hand, acetone exhibits a higher autoignition temperature (465 °C) [71], compared to that of cyclopentane (361 °C) [69], making it less susceptible to spontaneous combustion in maritime storage and transport conditions. Even though both acetone and cyclopentane are highly flammable, acetone has a broader flammable range in air (2.6%–12.8%) [71], in contrast to cyclopentane's narrower range (1.1%–8.7%) [69].

Finally, acetone stands out as one of the most widely used working fluids in ORC system studies [72–77], due to its favorable chemical properties, including thermal stability, low molecular weight, and suitable critical point constants [72]. Notably, Meziane et al. [43] reported a degradation temperature of 527 °C. Additionally, Davoud et al. [44] found that acetone degrades within a temperature range of 500–600 °C, decreasing to 462 °C with prolonged residence times, which remains well above typical operating conditions.

3.2. Sankey diagram

Fig. 6 shows a detailed Sankey diagram of the system evaluated in the case of full load operation. The diagram shows the main outgoing power flows from both diesel generators.

Approximately 45.3% of the energy released from the combustion of the fuel is converted into shaft power. The generator, with an efficiency of 98%, achieves a net electricity generation of 14,400 kWh, with 0.86% of the input energy flow constituting generator losses. Accordingly, the gross electrical efficiency of the diesel generator is 44.4%. From the cooling circuit, an output power of 1824 kW (5.6% of the input power) is obtained, resulting in 1550.4 kW of HSW in a heat exchanger, which is equivalent to 4.8% of the input energy flow.

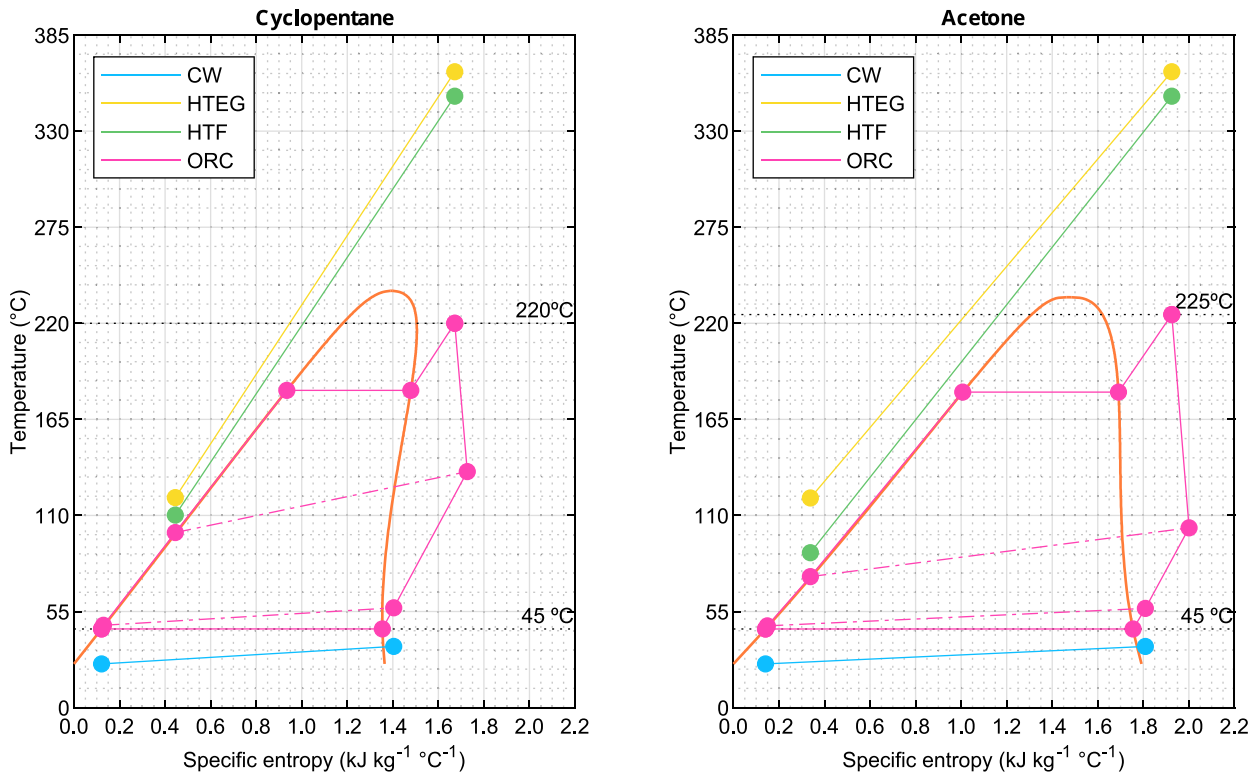

Fig. 5. *T-s* diagrams of the pre-selected organic working fluids.

The remaining input power of the generator is distributed as follows: 9.6% to a high-temperature charge air heat circuit, 4.7% to a low-temperature charge air heat circuit, 4.5% to a lubricating oil circuit, and 1.4% to radiation losses. Additionally, 28.9% of the fuel energy is transferred to the exhaust gases. The same energy flow distribution is applicable to the second diesel generator.

In the mixer, the two energy flows from the exhaust gases of the diesel generators are combined. This amounts to a total input energy flow of 18,732 kW to the integrated ORC system. This heat flow is considered as the reference value for evaluating the ORC system. The exhaust gases pass through the high-temperature heat exchanger (HTHX), transferring 65.4% of their energy to the heat transfer fluid. The remainder consists of losses in the HTHX (7.2%) and waste heat remaining in the exhaust gases (27.4%), as they leave the system at a temperature of 120 °C. Following this, the heat transfer fluid transfers the majority of its energy to acetone in the evaporator (58%), with the remaining 7.4% representing losses from the equipment. Moreover, the regenerator serves as a loop to enhance the system's energy before the working fluid enters the expander, transferring 5.9% of the energy from the fluid leaving the expander to the fluid exiting the pump. However, this process also entails losses within the regenerator, amounting to 0.65%. Consequently, the energy flow recovered from the organic fluid in the regenerator is 6.55%. In the condenser, 43.9% of the energy contained in the exhaust gases is transferred to the cooling seawater, with 2.3% representing heat losses to the environment. The expander extracts 2334.3 kW from the working fluid (12.5%), with mechanical losses and generator losses representing 0.37% and 0.36% of the input energy flow in the exhaust gas, respectively. Finally, the ORC system provides a gross electrical power output of 2195.4 kW (11.7%). The operation of the pump requires a power consumption of 91.97 kW. In the ORC system, this contributes 88.8 kW to increasing the enthalpy of the cold fluid before entering the regenerator, as a result of the pressure increase from 1 to 20 bar. Finally, the system produces a net AC power output of 30.9 MW.

When considering the input energy flow of both diesel generators as 100%, the system adds an additional 3.4% to the electrical power output, reaching a net electrical efficiency of the whole system ($\eta_{e,net}$) equal to 48.7%. This represents a reasonably high performance, since nearly half of the input energy flow to the system can be converted into electric power to supply the loads and the ship's propulsion system. Additionally, 3.1 MW of waste heat can be recovered through jacket cooling water heat exchangers for the production of HSW (4.8% of the input energy flow). Therefore, the CHP system allows reaching a net overall efficiency ($\eta_{CHP,net}$) of 53.5%.

For comparison, Herrera et al. [78] reported a thermodynamic efficiency (η_{ORC}) of approximately 22.5% for an ORC cycle using acetone, which is slightly higher than the thermodynamic efficiency of 19.1% achieved in the present study. This slight difference is attributed to the higher evaporator pressure of 24 bar adopted in the study by Herrera et al. [78] compared to the maximum pressure of 20 bar used in this work. By contrast, Pantaleo et al. [39] reported a thermodynamic efficiency of 15% under operating conditions of 24.9 bar and a condensation pressure of 1.13 bar. Furthermore, the expander efficiency in that study was 64%. Despite this, the expander efficiency of 85% used here is frequently cited in the literature. Although Choudhary et al. [79] assumed a higher isentropic efficiency of 90%, most authors typically report lower isentropic efficiencies of around 85%, [27,53–56].

3.3. Off-design performance of the integrated organic Rankine cycle unit

In order to evaluate the behavior of the system under real operating conditions, an ORC unit designed to operate with acetone and optimized for 85% load of the port engines is analyzed in this section. The term "off-design" refers to operating conditions that do not match the optimal parameters established during the system's design [80–82]. This concept is key to understanding how the ORC responds when operating outside its ideal range, which can affect its efficiency, performance, and reliability. Analyzing these off-design conditions is essential to optimize performance in various operational scenarios and to ensure the system's safety and adaptability to changes in the environment or load.

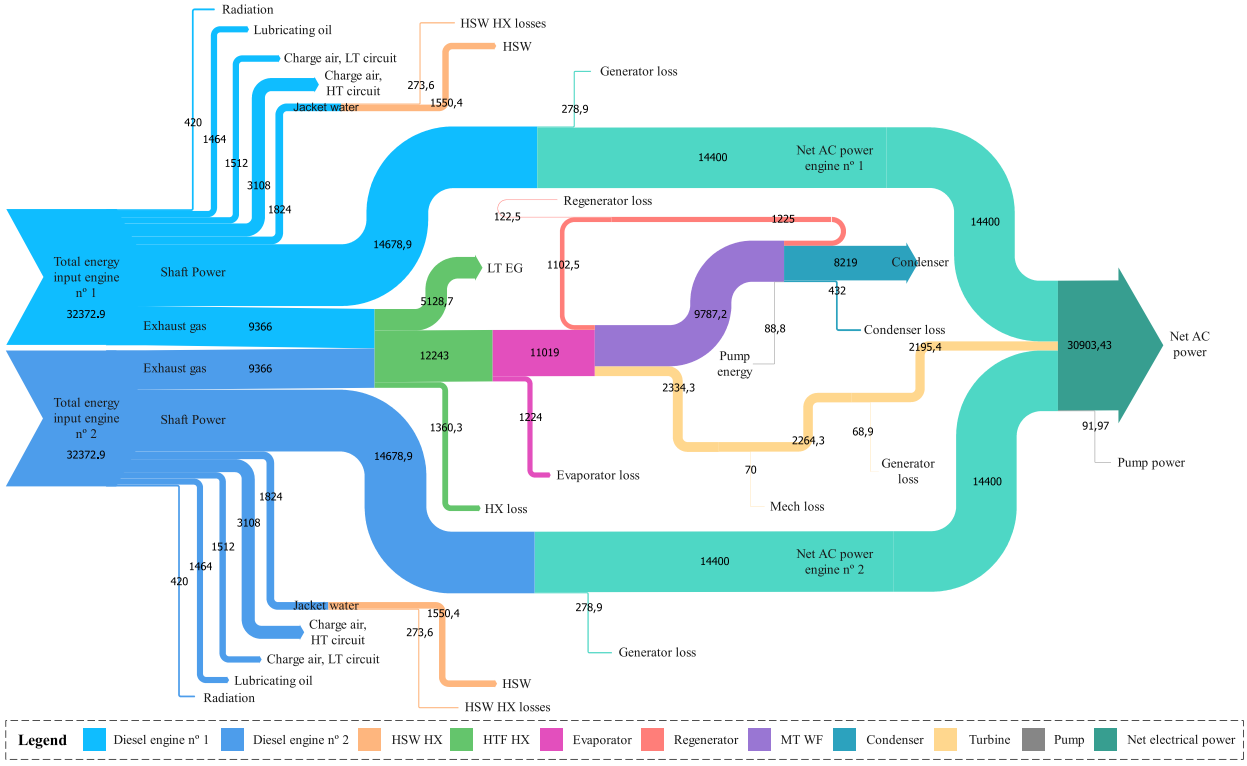

Fig. 6. Sankey diagram of the marine diesel engine and ORC system under full load operation.

Fig. 7 provides a comprehensive analysis of the performance of the diesel generator and ORC bottoming unit under different off-design conditions.

Fig. 7(*a*) illustrates the relationship between the exhaust gas energy flow and the net power output of the ORC system and the diesel generator. For the diesel generator, a linear trend is evident, indicating a direct increase in power output with rising exhaust gas energy flow. However, the net power output of the ORC system follows a less straightforward trend.

Fig. 7(*b*) shows various efficiencies of the bottoming power unit as a function of the exhaust gas energy flow. The efficiency of the HTHX (η_{htf}) remains relatively stable around 18.5%–19%, indicating consistent performance of the HTHX at varying loads. By contrast, the efficiency of the bottoming power unit (η_{bottom}) exhibits a slightly higher increase with the rise in exhaust gas energy flow, reaching values close to 8%.

Fig. 7(*c*) presents the minimum specific fuel oil consumption (SFOC) of multiple diesel generators operating simultaneously for varying power loads. Variations in SFOC are observed with changes in generator power, displaying a stepped behavior that reflects different operational zones depending on the number of generators in operation. As the number of simultaneously operating diesel generators increases, the total power delivered by the diesel generators rises, and the SFOC shows a slight increasing trend.

Finally, 7(*d*) represents the exhaust gas temperature and flow rate of various diesel generators (DGs) operating simultaneously. Temperature variations in the exhaust gases are observed when operating with one or a combination of engines. When using a single engine up to 50% load, the temperature remains below 297 °C. However, as the diesel generator load increases beyond 50%, the exhaust temperature progressively rises, reaching 364 °C at full load. Operating multiple engines simultaneously results in a higher exhaust gas flow rate, which in turn stabilizes the exhaust gas temperature. The increased flow rate provides more energy, leading to enhanced performance of the ORC system and improving overall system efficiency. By contrast, when operating with a single engine, load variations have a greater influence on the exhaust gas temperature. However, with the simultaneous operation of several diesel generators, the exhaust gas temperature becomes more stable, and small load variations have a reduced impact on the exhaust gas temperature.

3.4. Route performance

Baldi et al. [83] conducted a detailed analysis of the energy performance of a cruise ship operating in the Baltic Sea using operational data measured over one year. The ship's propulsion system includes two propulsion lines, each with two four-stroke Wärtsilä diesel engines, and propulsion accounts for 70% of annual energy consumption. However, the ship's maximum speed is rarely utilized, and most of the time, only one or two engines are operating simultaneously [83]. For this reason, in this work the ORC system has been evaluated with acetone as working fluid at 85% load of the port diesel generators. Baldi et al. [83] reported that electricity and heat demands are approximately 10% and 20% of the total energy consumption, respectively, supporting systems such as high-temperature heat recovery, steam systems, auxiliary boilers, and various electrical consumers. The route data provided by Baldi et al. [83] were adjusted to match the system's nominal power for optimization, aiming to minimize diesel consumption and maximize ORC usage to meet electrical demands. The operation of diesel generators and the ORC system was simulated using the results obtained from the off-design study (Section 3.3).

Fig. 8 shows the distribution of instantaneous power demand and generation on a ship over four typical days spanning different seasons, detailing the contributions of the port and starboard diesel generators, as well as the ORC system.

Over the four days, power demand varies significantly, influencing the operation of port and starboard diesel generators and the ORC system. On Day 1, demand fluctuates between 5 MW and 20 MW, managed by port diesel generators, with the ORC system contributing steadily but shutting down when the engine load drops below 50%

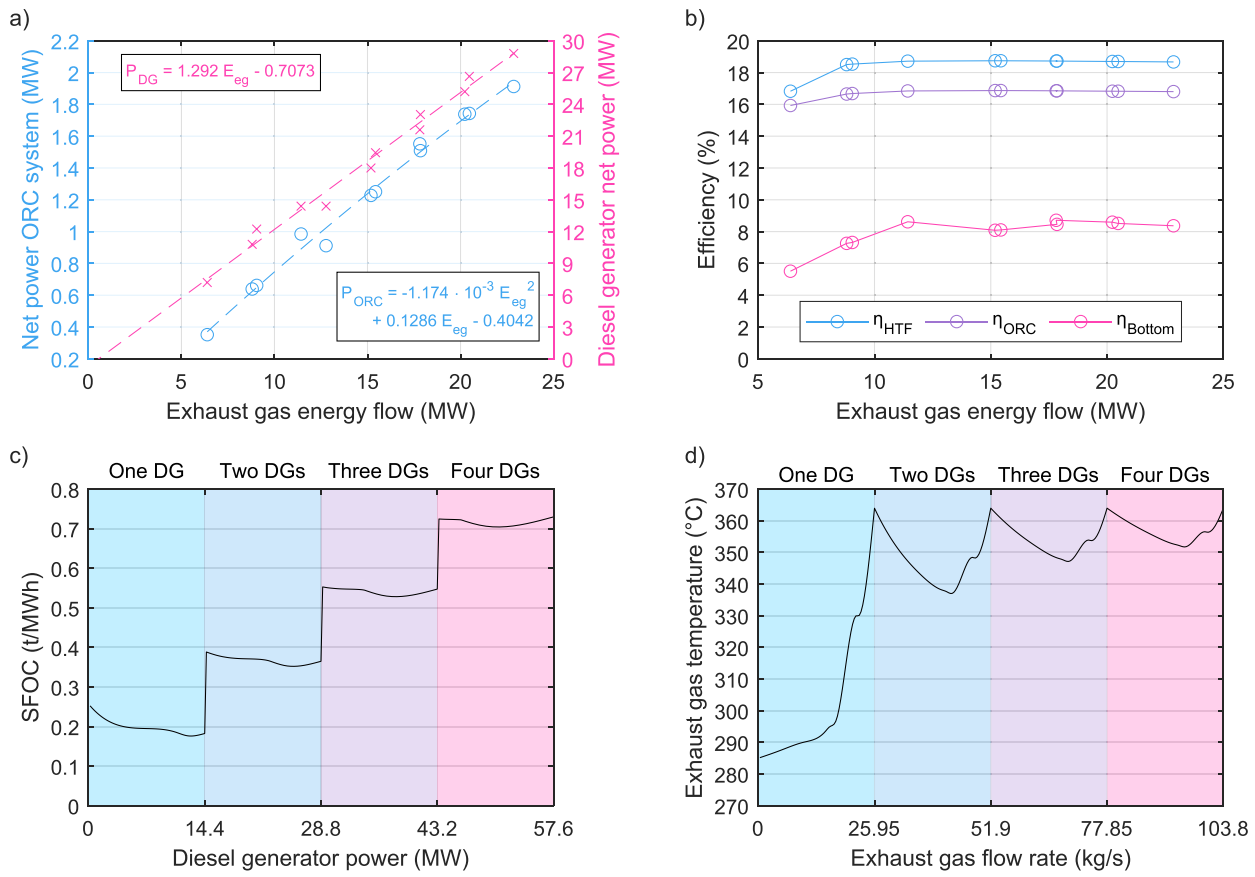

Fig. 7. (*a*) Net power of the ORC system and diesel generators in off-design mode as a function of the exhaust gas energy flow, (*b*) ORC system efficiencies in off-design mode as a function of the exhaust gas energy flow, (*c*) Minimum SFOC curve of various diesel generators (DGs) operating simultaneously for different powers served, and (*d*) Exhaust gas temperature and flow rate of various diesel generators (DGs) operating simultaneously.

Table 7
Total energy generation, diesel consumption and CO_2 emissions of the vessel by route.

Case	Component	Total energy generated (MWh)				Diesel consumption (t)				CO_2 emisions (t)			
		Day 1	Day 2	Day 3	Day 4	Day 1	Day 2	Day 3	Day 4	Day 1	Day 2	Day 3	Day 4
1	Port diesel generators	274.43	376.45	328.34	261.54	5.84	6.48	6.07	5.67	18.57	20.56	19.27	18.03
	Startboard diesel generators	0	216.00	58.43	0								
	ORC System	16.15	23.43	20.07	15.04	0	0	0	0	0	0	0	0
2	Base case (4xWärtsilä 12V46F)	291.97	616.64	408.22	277.92	6.27	10.16	7.02	6.06	19.91	32.26	22.27	19.23

between 16 h and 20 h. Day 2 starts with high demand (45–50 MW), which drops to 5 MW and stabilizes at 10–15 MW, leading both port and starboard generators to adjust accordingly. The ORC system operates consistently until 11 h but shuts down until 18 h due to low engine load. Day 3 sees an initial demand of 10 MW, peaking at 45 MW around 20 h, prompting the activation of starboard generators as demand exceeds 30 MW, while the ORC system maintains a low, constant contribution. On Day 4, demand fluctuates between 5 MW and 20 MW with multiple peaks, managed by port generators, and the ORC system provides minimal output, shutting down when the engine load falls below 50%.

Table 7 presents the cumulative data for each of the days analyzed. In particular, the analysis indicates an average daily reduction in diesel consumption by 1.4 tonnes, resulting in a daily decrease of 4.4 tonnes of CO_2 emissions, considering that the fuel contains 86.6% carbon [84]. Extrapolating these data over an annual period, the implementation of the ORC system would reduce diesel consumption and CO_2 emissions by 18.5%. These values are comparable to those presented by Bouman et al. [85] and Baldasso et al. [86], who suggested that the installation of WHR units on board vessels could lead to a reduction in CO_2 emissions in the range of 1% to 20%.

3.5. Economic feasibility assessment

The capital cost of the ORC unit was determined using the correlations previously reported in Table 5, adjusted using the CEPCI to the current year. Accordingly, the PEC of the ORC in 2024 is estimated to be approximately \$1490/kW_e. To provide context, Pantaleo et al. [39] conducted a thermoeconomic optimization study on small-scale ORC systems designed for WHR. They evaluated 18 organic working fluids and found power capital costs in the range of \$2000–5000/kW_e. It is noteworthy that the power capital cost of an ORC unit generally decreases with an increase in electrical power output [87]. Accordingly, for systems with relatively high electrical power outputs (> 1 MW_e), the power capital cost is typically lower than €3000/kW_e [87]. Girgin et al. [88] also reported that the cost of various ORC systems from different manufacturers for naval applications ranges from \$1800 to \$2857 per kW.

3.5.1. Baseline assessment

The following assumptions have been made for the techno-economic assessment of the baseline scenario.

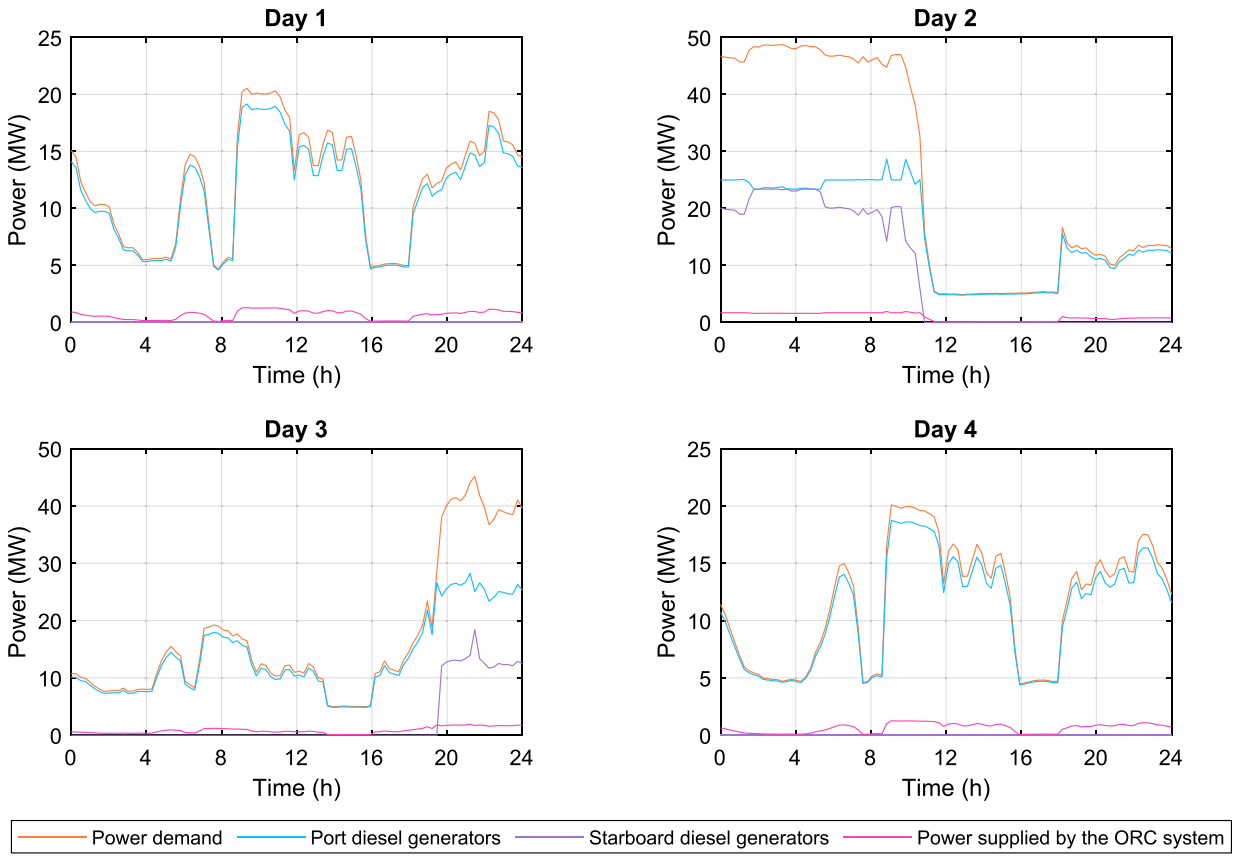

Fig. 8. Route performance on various typical days.

- Based on the findings reported in Table 5, average daily savings of 2.5 tonnes of diesel fuel are considered.
- The density of marine diesel fuel is estimated at 900 kg/m^3 [93].
- An average diesel price of $0.85 per liter is assumed, based on the latest data (between 2020 and 2024) from the ANAVE (Spanish Shipping Association) [94].
- Direct and indirect fixed-capital investment costs as a percentage of the PEC are provided in the literature [58,89,90]. Table 8 shows a breakdown of all costs associated with the project. The installation of an ORC unit of 1.6 MW_e requires a capital investment of $7,203,700, which constitutes an approximate capital cost value of $4500/$kW_e$.
- For the operational and maintenance (O&M) costs of the ORC system equipment, a conservative estimate of 20% of the total PEC price is assumed [57]. In related studies, Gomaa et al. [91] suggested O&M values over the project's lifespan, with 4% for heat exchangers and 2% for the pump and expander, based on the PEC price. Additionally, Pallis et al. [21] indicated an annual O&M cost of 2% of the PEC.
- For vessel operation, a shipping time of 8640 h per year (approximately 360 days) is assumed. For comparison, Lion et al. [52] reported 340 days of operation, typical for a chemical tanker making 8 voyages per year from Dubai to Hamburg.
- The project lifespan is assumed to be 25 years [86,95]. A relatively lower lifespan of 20 years has been assumed in related works [21,96,97].
- A rather conservative discount rate (interest rate) of 8% has been assumed [21]. For context, lower discount rates of 5% were considered in related studies by Shu et al. [98], Wang et al. [99] and Konur et al. [96]; while a discount rate of 6% was assumed by Baldasso et al. [95]. By contrast, Ahmed et al. [100] and Habibi et al. [97] reported a higher value of 10% for the discount rate.

For the project baseline values, using a WACC of 0.08, it is expected that the investment will be recovered in 11.7 years, according to the discounted payback method (DPB). The net present value (NPV) over the project lifespan of 25 years is $3,165,600, yielding an internal rate of return (IRR) of 0.128. Furthermore, a profitability index (PI) of 44% is obtained, i.e., an accumulated profit of up to 44% based on the initial investment.

3.5.2. *Sensitivity analysis*

A sensitivity analysis of the NPV for various values of the WACC ranging from 0 to 0.20 is illustrated in Fig. 9. As the IRR is equal to 0.128, the investment is profitable only for WACC values below 0.128. The project achieves a benefit higher than the initial investment, indicated by a PI greater than unity, when the WACC is below 0.05.

Fig. 10 presents a sensitivity analysis of several key factors influencing the installation of an ORC system onboard a shuttle tanker ship. The analysis examines the impacts of diesel price, government subsidy percentage, CO_2 emissions price, and utilization factor on various economic indicators.

Firstly, the effect of the utilization factor, measured in days, is evaluated. As the utilization factor increases from 290 to 360 days, the discounted payback period decreases from around 17.5 years to approximately 11.5 years. The NPV shows can reach approximately $3.2M with higher utilization. Likewise, the PI rises from around 0.16 to 0.44, and the IRR improves slightly from approximately 0.1 to 0.13. A high utilization factor leads to better economic outcomes, but is not a particularly influential parameter within the range of values examined.

The second parameter considered is the price of CO_2 emissions. As the price of CO_2 emissions rises from $0 per tonne to $175 per tonne, the discounted payback period decreases from about 15.5 years to approximately 9.5 years. Correspondingly, the NPV increases from around $1.7M to $4.6M, reflecting the advantageous economic impact

Table 8
Cost breakdown of installing an ORC bottoming unit (1.6 MW_e) to recover waste heat from Wärtsilä 12V46F diesel generators for additional power generation.

Cost breakdown	Percentage range	Applied percentage	Cost estimate ($)
Fixed-capital investment (FCI)			**$6,244,900**
Direct fixed-capital investment (DFCI)			**$5,027,300**
Purchased-equipment cost (PEC)	N/A	N/A	$2,382,600
Purchased-equipment installation	45% of PEC [89] 30% of PEC [58] 50% of PEC [90]	40% of PEC	$ 953,050
Piping	31% of PEC [89] 20% of PEC [58] 30% of PEC [90] 9% of PEC [91]	27% of PEC	$643,310
Instrumentation and control	10% of PEC [89] 10% of PEC [58] 20% of PEC [90] 5% of PEC [91]	12% of PEC	$285,920
Electrical equipment and materials	10% of PEC [89] 10% of PEC [58]	10% of PEC	$238,260
Structural and architectural work	10% of PEC [89] 15% of PEC [58]	12% of PEC	$285,920
Service facilities	10% of PEC [89]	10% of PEC	$238,260
Indirect fixed-capital investment (IFCI)			**$1,217,500**
Engineering and supervision	30% of PEC [89] 25% of PEC [58] 50% of PEC [90]	30% of PEC	$714,790
Construction costs (including contractor's profit)	10% of DFCI [89]	10% of DFCI	$502,730
Other outlays			**$958,820**
Contingencies	10% of FCI [89] 20% of PEC [58]	20% of PEC	$476,530
Startup costs and working capital	10% of FCI [39,89] 10% of PEC [92] 20% of PEC [58]	15% OF PEC	$357,390
Legal costs	2% of FCI [89]	2% of FCI	$124,900
Total capital investment			**$7,203,700**

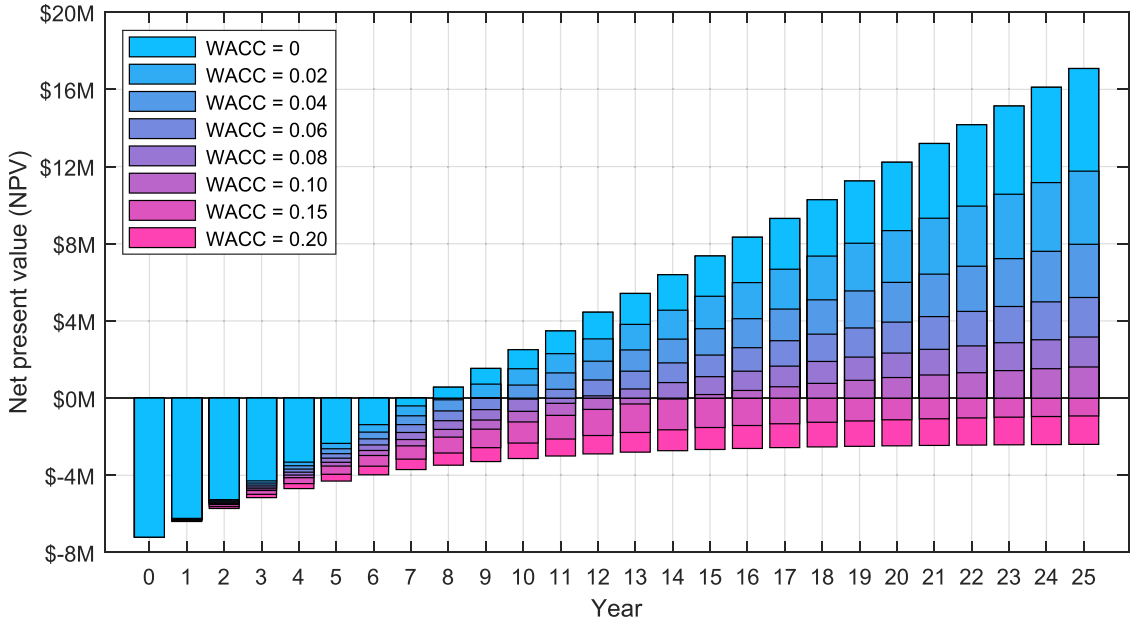

Fig. 9. Sensitivity analysis for different values of the WACC.

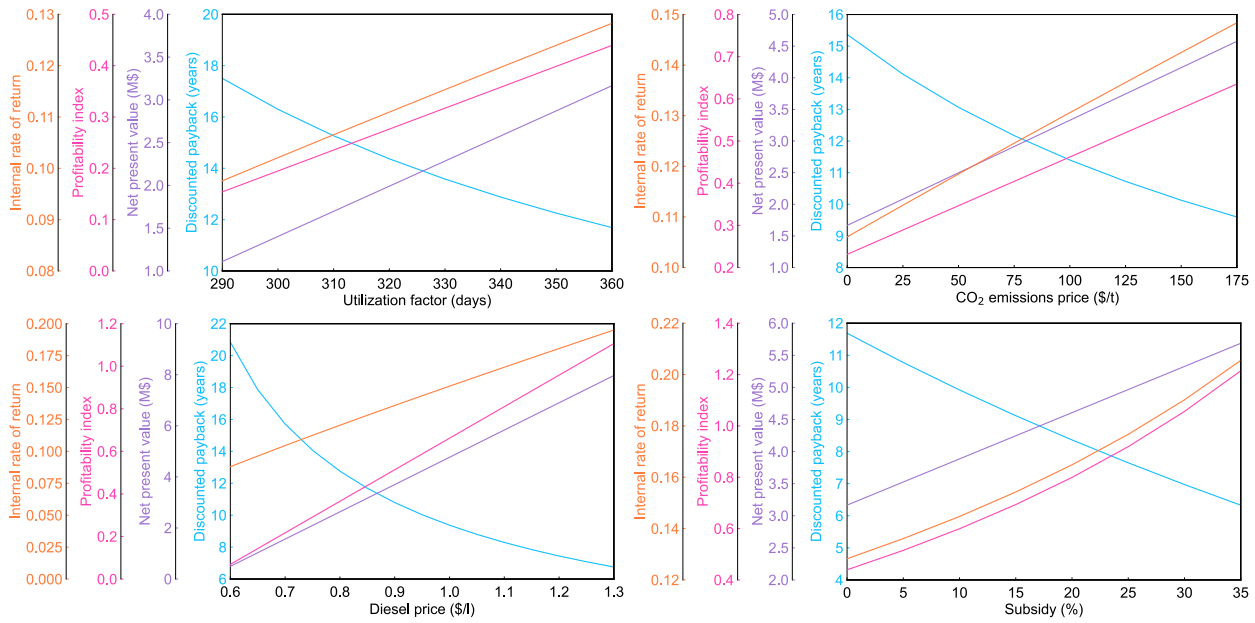

Fig. 10. Sensitivity assessment of the different economic parameters as a function of the diesel price (*top*), biomass price (*center*) and percentage of subsidy (*bottom*).

of higher CO_2 prices. The PI also increases from 0.23 to about 0.64 with the rise in CO_2 price. Similarly, the IRR improves from approximately 0.1 to 0.15, indicating that higher CO_2 prices make the investment more financially attractive.

The third parameter considered is the diesel price, which is a critical variable substantially affecting the economic performance of the ORC system. As the diesel price increases from $0.6 per liter to $1.3 per liter, the discounted payback period decreases sharply from approximately 20.8 years to around 6.7 years. Concurrently, the NPV shows a notable increase from $0.5M to about $8M. The PI also rises drastically from 0.07 to around 1.1 as the diesel price increases, indicating an accumulated profit of up to 110% based on the initial investment. Additionally, the IRR remarkably improves from 0.09 to approximately 0.2 with the rising diesel price, highlighting enhanced project viability under higher diesel costs.

The last parameter analyzed is the percentage of non-refundable subsidies on the capital investment. Increasing the subsidy from 0% to 35% significantly reduces the discounted payback period from approximately 11.7 years to around 6.3 years. Similarly, the NPV increases from roughly $3.2M to $5.7M with higher subsidy rates. The PI exhibits a substantial increase from around 0.44 to 1.21 as the subsidy percentage rises. Furthermore, the IRR improves from 0.13 to 0.21, demonstrating the beneficial impact of subsidies on the project's financial performance.

4. Conclusion

This study has demonstrated the techno-economic viability of implementing a regenerative ORC cycle for waste heat recovery from marine diesel engines using acetone as the working fluid. The system is designed to generate an additional 2.2 MW_e of electric power from the thermal energy contained in the exhaust gases of two diesel generators with 14.4 MW_e each of nominal electric power installed on board a DC cargo distribution vessel. The key conclusions derived from this study are presented in the following points:

- Considering the overall energy performance of the system, it achieves a net overall electrical efficiency of 48.7%, meaning nearly half of the input energy is converted into electrical power to supply the loads and propulsion system. Additionally, 3.1 MW of waste heat (4.8% of the input energy) is recovered through engine jacket water heat exchangers for the production of HSW, enabling the CHP system to reach a net overall efficiency of 53.5%. At 85% generator load, the system demonstrates a net electrical efficiency of 8.45% and a thermodynamic efficiency of 18.73%.
- Implementing this technology in a DC distribution vessel results in a significant reduction in CO_2 emissions. It is estimated that adopting the ORC system could achieve an annual decrease of 18.5% in CO_2 emissions and diesel consumption compared to a reference scenario without this technology.
- The financial analysis indicates that the ORC provides a cumulative return on investment of 44%, with a payback period of 11.7 years and an internal rate of return of 12.8%, suggesting it could be a worthwhile investment, particularly when considering potential incentives for carbon reduction and subsidy.
- By reducing diesel consumption, the ORC system mitigates the financial impact of fuel price fluctuations, which is particularly relevant for maritime operations where fuel costs represent a significant portion of total operating expenses. The system offers a strategic advantage in an industry increasingly affected by rising fuel prices and stricter emissions regulations.

The comprehensive evaluation of the ORC unit presented in this study, including energy analysis, economic and environmental assessments, off-design optimization using real ship routes, as well as a detailed sensitivity analysis, fills a significant gap in the literature. By integrating technical performance, economic viability, and environmental impact, this approach provides a holistic and practical perspective that is essential for real-world applications. The inclusion of off-design optimization with real ship routes ensures that the system's performance is accurately assessed under varying operational conditions, making this research particularly valuable for the maritime sector. These insights are key in guiding the adoption of ORC technology in actual marine operations, offering a pathway to more efficient, cost-effective, and environmentally sustainable solutions in the industry.

CRediT authorship contribution statement

Daniel Sánchez-Lozano: Writing – review & editing, Writing – original draft, Visualization, Validation, Software, Methodology, Investigation, Formal analysis, Data curation, Conceptualization. **Roque**

Aguado: Writing – review & editing, Writing – original draft, Visualization, Validation, Methodology, Investigation, Formal analysis, Conceptualization. **Antonio Escámez:** Writing – review & editing, Visualization, Software, Methodology, Investigation, Formal analysis, Conceptualization. **José Antonio Hernández-Torres:** Visualization, Resources, Methodology, Investigation, Conceptualization. **Juan P. Torreglosa:** Validation, Supervision, Resources, Project administration, Methodology, Investigation, Funding acquisition, Conceptualization. **David Vera:** Validation, Supervision, Project administration, Methodology, Investigation, Funding acquisition, Conceptualization.

Funding

This work was supported in part by "Programa Operativo FEDER 2014-2020" and "Consejería de Economía, Conocimiento, Empresas *y* Universidad de la Junta de Andalucía" under Project UHU-202051 and in part by CEI·MAR through the scientific improvement axis of the CEI·MAR 2023 Plan: Research Projects of early-career Ph.D. CEI·MAR 2023 under Project CEI-JD-12.

Roque Aguado, Antonio Escámez and Daniel Sánchez acknowledge financial support from Ministerio de Ciencia, Innovación *y* Universidades under the FPU Program (Refs. FPU19/00930, FPU22/00741, FPU22/00879, respectively).

Declaration of competing interest

The authors declare that they have no known competing financial interests or personal relationships that could have appeared to influence the work reported in this paper.

Data availability

Data will be made available on request.

References

[1] Soffiato M, Frangopoulos CA, Manente G, Rech S, Lazzaretto A. Design optimization of ORC systems for waste heat recovery on board a LNG carrier. Energy Convers Manag 2015;92:523–34. http://dx.doi.org/10.1016/j.enconman.2014.12.085.

[2] IRENA. A pathway to decarbonise the shipping sector by 2050. Tech. rep., IRENA; 2021.

[3] IMO. Fourth IMO GHG study. Tech. rep., IMO (International Maritime Organization); 2020.

[4] Roslan SB, Konovessis D, Tay ZY. Sustainable hybrid marine power systems for power management optimisation: A review. Energies 2022;15(24). http://dx.doi.org/10.3390/en15249622.

[5] Zahedi B, Norum LE, Ludvigsen KB. Optimized efficiency of all-electric ships by DC hybrid power systems. J Power Sources 2014;255:341–54. http://dx.doi.org/10.1016/j.jpowsour.2014.01.031.

[6] Micheli D, Clemente S, Taccani R. Chapter 2 - energy systems on board ships. In: Baldi F, Coraddu A, Mondejar ME, editors. Sustainable energy systems on ships. Elsevier; 2022, p. 27–78. http://dx.doi.org/10.1016/B978-0-12-824471-5.00008-6.

[7] Haseltalab A, Botto MA, Negenborn RR. Model predictive DC voltage control for all-electric ships. Control Eng Pract 2019;90:133–47. http://dx.doi.org/10.1016/j.conengprac.2019.06.018.

[8] Haseltalab A, Wani F, Negenborn RR. Multi-level model predictive control for all-electric ships with hybrid power generation. Int J Electr Power Energy Syst 2022;135:107484. http://dx.doi.org/10.1016/j.ijepes.2021.107484.

[9] Nuchturee C, Li T, Xia H. Energy efficiency of integrated electric propulsion for ships – A review. Renew, Sust, Energ, Rev 2020;134:110145. http://dx.doi.org/10.1016/j.rser.2020.110145.

[10] Geertsma R, Negenborn R, Visser K, Hopman J. Design and control of hybrid power and propulsion systems for smart ships: A review of developments. Appl Energy 2017;194:30–54. http://dx.doi.org/10.1016/j.apenergy.2017.02.060.

[11] Singh DV, Pedersen E. A review of waste heat recovery technologies for maritime applications. Energy Convers Manag 2016;111:315–28. http://dx.doi.org/10.1016/j.enconman.2015.12.073.

[12] Sellers C. Field operation of a 125kW ORC with ship engine jacket water. Energy Procedia 2017;129:495–502. http://dx.doi.org/10.1016/j.egypro.2017.09.168, 4th International Seminar on ORC Power SystemsSeptember 13-15th 2017 POLITECNICO DI MILANOBOVISA CAMPUSMILANO, ITALY.

[13] Pili R, Romagnoli A, Kamossa K, Schuster A, Spliethoff H, Wieland C. Organic Rankine Cycles (ORC) for mobile applications – Economic feasibility in different transportation sectors. Appl Energy 2017;204:1188–97. http://dx.doi.org/10.1016/j.apenergy.2017.04.056.

[14] Mondejar ME, Ahlgren F, Thern M, Genrup M. Quasi-steady state simulation of an organic Rankine cycle for waste heat recovery in a passenger vessel. Appl Energy 2017;185:1324–35. http://dx.doi.org/10.1016/j.apenergy.2016.03.024, Clean, Efficient and Affordable Energy for a Sustainable Future.

[15] Casisi M, Pinamonti P, Reini M. Increasing the energy efficiency of an internal combustion engine for ship propulsion with bottom ORCs. Appl Sci 2020;10(19).

[16] Mat Nawi Z, Kamarudin S, Sheikh Abdullah S, Lam S. The potential of exhaust waste heat recovery (WHR) from marine diesel engines via organic rankine cycle. Energy 2019;166:17–31. http://dx.doi.org/10.1016/j.energy.2018.10.064.

[17] Song J, Song Y, wei Gu C. Thermodynamic analysis and performance optimization of an Organic Rankine Cycle (ORC) waste heat recovery system for marine diesel engines. Energy 2015;82:976–85. http://dx.doi.org/10.1016/j.energy.2015.01.108.

[18] Catapano F, Frazzica A, Freni A, Manzan M, Micheli D, Palomba V, et al. Development and experimental testing of an integrated prototype based on Stirling, ORC and a latent thermal energy storage system for waste heat recovery in naval application. Appl Energy 2022;311:118673. http://dx.doi.org/10.1016/j.apenergy.2022.118673.

[19] Konur O, Yuksel O, Aykut Korkmaz S, Ozgur Colpan C, Saatcioglu OY, Koseoglu B. Operation-dependent exergetic sustainability assessment and environmental analysis on a large tanker ship utilizing Organic Rankine cycle system. Energy 2023;262:125477. http://dx.doi.org/10.1016/j.energy.2022.125477.

[20] Yang M-H, Yeh R-H. Thermodynamic and economic performances optimization of an organic Rankine cycle system utilizing exhaust gas of a large marine diesel engine. Appl Energy 2015;149:1–12. http://dx.doi.org/10.1016/j.apenergy.2015.03.083.

[21] Pallis P, Varvagiannis E, Braimakis K, Roumpedakis T, Leontaritis AD, Karellas S. Development, experimental testing and techno-economic assessment of a fully automated marine organic rankine cycle prototype for jacket cooling water heat recovery. Energy 2021;228:120596. http://dx.doi.org/10.1016/j.energy.2021.120596.

[22] Zeng J, Chen W, Yu W, Lyu L, Luo W, Xue S. Application analysis of organic Rankine cycle technology to recover ship waste heat and construction of experimental bench. In: 2022 7th international conference on power and renewable energy. 2022, p. 1063–8. http://dx.doi.org/10.1109/ICPRE55555.2022.9960614.

[23] Ng C, Tam ICK, Wu D. Thermo-economic performance of an organic Rankine cycle system recovering waste heat onboard an offshore service vessel. J Mar Sci Eng 2020;8(5). http://dx.doi.org/10.3390/jmse8050351.

[24] Doerry N, Amy J. MVDC shipboard power system considerations for electromagnetic railguns. 2015.

[25] Torreglosa JP, López-García D, Hernández-Torres J, Vera D, Vallés AP, Clavijo-Camacho J. MVDC electric propulsion systems for integrating waste heat recovery systems in marine transport. IEEE Trans Transp Electrif. 2024. http://dx.doi.org/10.1109/TTE.2024.3356655, 1–1.

[26] Wärtsilä. Wärtsilä 46F product guide. Tech. rep., Wärtsilä; 2020.

[27] Aguado R, Baccioli A, Liponi A, Vera D. Continuous decentralized hydrogen production through alkaline water electrolysis powered by an oxygen-enriched air integrated biomass gasification combined cycle. Energy Convers Manag 2023;289:117149. http://dx.doi.org/10.1016/j.enconman.2023.117149.

[28] Vera D, Jurado F, Carpio J, Kamel S. Biomass gasification coupled to an EFGT-ORC combined system to maximize the electrical energy generation: A case applied to the olive oil industry. Energy 2018;144:41–53. http://dx.doi.org/10.1016/j.energy.2017.11.152.

[29] Mana A, Kaitouni S, Kousksou T, Jamil A. Enhancing sustainable energy conversion: Comparative study of superheated and recuperative ORC systems for waste heat recovery and geothermal applications, with focus on 4E performance. Energy 2023;284:128654. http://dx.doi.org/10.1016/j.energy.2023.128654.

[30] de Mena B, Vera D, Jurado F, Ortega M. Updraft gasifier and ORC system for high ash content biomass: A modelling and simulation study. Fuel Process Technol 2017;156:394–406. http://dx.doi.org/10.1016/j.fuproc.2016.09.031.

[31] Bahrami M, Pourfayaz F, Kasaeian A. Low global warming potential (GWP) working fluids (WFs) for Organic Rankine Cycle (ORC) applications. Energy Rep 2022;8:2976–88. http://dx.doi.org/10.1016/j.egyr.2022.01.222.

[32] Douvartzides S, Karmalis I. Working fluid selection for the Organic Rankine Cycle (ORC) exhaust heat recovery of an internal combustion engine power plant. IOP Conf Ser: Mater Sci Eng 2016;161(1):012087. http://dx.doi.org/10.1088/1757-899X/161/1/012087.

[33] Ge Z, Li J, Duan Y, Yang Z, Xie Z. Thermodynamic performance analyses and optimization of dual-loop organic Rankine cycles for internal combustion engine waste heat recovery. Appl Sci 2019;9(4).

[34] National Fire Protection Association. NFPA 704 Standard System for the Identification of the Hazards of Materials for Emergency Response.

[35] Luo D, Mahmoud A, Cogswell F. Evaluation of low-GWP fluids for power generation with organic rankine cycle. Energy 2015;85:481–8. http://dx.doi.org/10.1016/j.energy.2015.03.109.

[36] Drescher U, Brüggemann D. Fluid selection for the Organic Rankine Cycle (ORC) in biomass power and heat plants. Appl Therm Eng 2007;27(1):223–8. http://dx.doi.org/10.1016/j.applthermaleng.2006.04.024.

[37] Bao J, Zhao L. A review of working fluid and expander selections for organic Rankine cycle. Renew Sust. Energ Rev 2013;24:325–42. http://dx.doi.org/10.1016/j.rser.2013.03.040.

[38] Thermoflow inc. 2024, Available online: https://www.thermoflow.com/index.html. [Accessed 5 January 2024].

[39] Pantaleo A, Simpson M, Rotolo G, Distaso E, Oyewunmi O, Sapin P, et al. Thermoeconomic optimisation of small-scale organic Rankine cycle systems based on screw vs. piston expander maps in waste heat recovery applications. Energy Convers Manag 2019;200:112053. http://dx.doi.org/10.1016/j.enconman.2019.112053.

[40] Köse Ö, Koç Y, Yağlı H. Performance improvement of the bottoming steam Rankine cycle (SRC) and organic Rankine cycle (ORC) systems for a triple combined system using gas turbine (GT) as topping cycle. Energy Convers Manag 2020;211:112745. http://dx.doi.org/10.1016/j.enconman.2020.112745.

[41] US Environmental Protection Agency. Transitioning to low-GWP alternatives. Tech. rep., U.S. Environmental Protection Agency; 2016.

[42] Dai X, Shi L, Qian W. Review of the working fluid thermal stability for organic rankine cycles. J Therm Sci 2019;28(4):597–607. http://dx.doi.org/10.1007/s11630-019-1119-3.

[43] Meziane I, Fenard Y, Delort N, Herbinet O, Bourgalais J, Ramalingam A, et al. Experimental and modeling study of acetone combustion. Combust Flame 2023;257:112416. http://dx.doi.org/10.1016/j.combustflame.2022.112416, James A. Miller Special Commemorative Issue.

[44] Davoud JG, Hinshelwood CN. Thermal decomposition of acetone. Nature 1939;144(3656):909–10. http://dx.doi.org/10.1038/144909a0.

[45] Lebedevas S, Čepaitis T. Complex use of the main marine diesel engine high- and low-temperature waste heat in the organic Rankine cycle. J Mar Sci Eng 2024;12(3). http://dx.doi.org/10.3390/jmse12030521.

[46] Sánchez-Lozano D, Escámez A, Aguado R, Oulbi S, Hadria R, Vera D. Techno-economic assessment of an off-grid biomass gasification CHP plant for an olive oil mill in the region of Marrakech-Safi, Morocco. Appl Sci 2023;13(10). http://dx.doi.org/10.3390/app13105965.

[47] Bianchi M, Branchini L, De Pascale A, Melino F, Orlandini V, Peretto A, et al. Techno-economic analysis of ORC in gas compression stations taking into account actual operating conditions. Energy Procedia 2017;129:543–50. http://dx.doi.org/10.1016/j.egypro.2017.09.182.

[48] Reis MML, Gallo WL. Study of waste heat recovery potential and optimization of the power production by an organic Rankine cycle in an FPSO unit. Energy Convers Manag 2018;157:409–22. http://dx.doi.org/10.1016/j.enconman.2017.12.015.

[49] Kim J-S, Kim D-Y. Energy, exergy, and economic (3E) analysis of SOFC-GT-ORC hybrid systems for ammonia-fueled ships. J Mar Sci Eng 2023;11(11).

[50] Chen W, Fu B, Zeng J, Luo W. Research on the operational performance of oganic Rankine cycle system for waste heat recovery from large ship main engine. Appl Sci 2023;13(14). http://dx.doi.org/10.3390/app13148543.

[51] Kosmadakis G, Neofytou P. Reversible high-temperature heat pump/ORC for waste heat recovery in various ships: A techno-economic assessment. Energy 2022;256:124634. http://dx.doi.org/10.1016/j.energy.2022.124634.

[52] Lion S, Taccani R, Vlaskos I, Scrocco P, Vouvakos X, Kaiktsis L. Thermodynamic analysis of waste heat recovery using Organic Rankine Cycle (ORC) for a two-stroke low speed marine Diesel engine in IMO Tier II and Tier III operation. Energy 2019;183:48–60. http://dx.doi.org/10.1016/j.energy.2019.06.123.

[53] Astolfi M, Romano MC, Bombarda P, Macchi E. Binary ORC (Organic Rankine Cycles) power plants for the exploitation of medium–low temperature geothermal sources – Part B: Techno-economic optimization. Energy 2014;66:435–46. http://dx.doi.org/10.1016/j.energy.2013.11.057.

[54] Camporeale SM, Pantaleo AM, Ciliberti PD, Fortunato B. Cycle configuration analysis and techno-economic sensitivity of biomass externally fired gas turbine with bottoming ORC. Energy Convers Manag 2015;105:1239–50. http://dx.doi.org/10.1016/j.enconman.2015.08.069.

[55] Das P, Mondal D, Ashraful Islam M, Afroj Lily M. Thermodynamic performance evaluation of a solar powered Organic Rankine cycle (ORC) and dual cascading vapor compression cycle (DCVCC): Power generation and cooling effect. Energy Convers Manag X 2024;23:100662. http://dx.doi.org/10.1016/j.ecmx.2024.100662.

[56] Zhou X, Xin Z, Tang W, Sheng K, Wu Z. Comparative study for waste heat recovery in immersion cooling data centers with district heating and organic Rankine cycle (ORC). Appl Therm Eng 2024;242:122479. http://dx.doi.org/10.1016/j.applthermaleng.2024.122479.

[57] Zare V. A comparative exergoeconomic analysis of different ORC configurations for binary geothermal power plants. Energy Convers Manag 2015;105:127–38. http://dx.doi.org/10.1016/j.enconman.2015.07.073.

[58] Braimakis K, Charalampidis A, Karellas S. Techno-economic assessment of a small-scale biomass ORC-CHP for district heating. Energy Convers Manag 2021;247:114705. http://dx.doi.org/10.1016/j.enconman.2021.114705.

[59] Jang Y, Lee J. Optimizations of the organic Rankine cycle-based domestic CHP using biomass fuel. Energy Convers Manag 2018;160:31–47. http://dx.doi.org/10.1016/j.enconman.2018.01.025.

[60] Zhang S, Li L, Huo E, Yu Y, Huang R, Wang S. Parameters analysis and techno-economic comparison of various ORCs and sCO2 cycles as the power cycle of Lead–Bismuth molten nuclear micro-reactor. Energy 2024;295:131103. http://dx.doi.org/10.1016/j.energy.2024.131103.

[61] Akrami E, Chitsaz A, Nami H, Mahmoudi S. Energetic and exergoeconomic assessment of a multi-generation energy system based on indirect use of geothermal energy. Energy 2017;124:625–39. http://dx.doi.org/10.1016/j.energy.2017.02.006.

[62] Gholamian E, Habibollahzade A, Zare V. Development and multi-objective optimization of geothermal-based organic Rankine cycle integrated with thermoelectric generator and proton exchange membrane electrolyzer for power and hydrogen production. Energy Convers Manag 2018;174:112–25. http://dx.doi.org/10.1016/j.enconman.2018.08.027.

[63] Behzadi A, Gholamian E, Houshfar E, Habibollahzade A. Multi-objective optimization and exergoeconomic analysis of waste heat recovery from Tehran's waste-to-energy plant integrated with an ORC unit. Energy 2018;160:1055–68. http://dx.doi.org/10.1016/j.energy.2018.07.074.

[64] Mahmoudi S, Ghavimi A. Thermoeconomic analysis and multi objective optimization of a molten carbonate fuel cell – Supercritical carbon dioxide – Organic Rankine cycle integrated power system using liquefied natural gas as heat sink. Appl Therm Eng 2016;107:1219–32. http://dx.doi.org/10.1016/j.applthermaleng.2016.07.003.

[65] Roy D, Samanta S, Roy S, Smallbone A, Paul Roskilly A. Fuel cell integrated carbon negative power generation from biomass. Appl Energy 2023;331:120449. http://dx.doi.org/10.1016/j.apenergy.2022.120449.

[66] Baral S, Šebo J. Techno-economic assessment of green hydrogen production integrated with hybrid and organic rankine cycle (ORC) systems. Heliyon 2024;10(4):e25742. http://dx.doi.org/10.1016/j.heliyon.2024.e25742.

[67] Tanbar F, Febriyanto R, Ariyadi HM, Nugraha AD, Simaremare AA, Supriyanto E, et al. Techno-economic studies of low GWP-organic rankine cycle for low-level geothermal waste heat utilization in Remote Island of Indonesia. Case Stud Therm Eng 2025;65:105385. http://dx.doi.org/10.1016/j.csite.2024.105385.

[68] Australian Government Department of Climate Change, Energy, the Environment and Water. Acetone. 2025, Available online: https://www.dcceew.gov.au/environment/protection/npi/substances/fact-sheets/acetone. [Accessed 25 February 2025].

[69] NOAA (National Oceanic and Atmospheric Administration). Acetone CAMEO chemicals. 2025, Available online: https://cameochemicals.noaa.gov/chris/CYP.pdf. [Accessed 25 February 2025].

[70] International Labour Organization (ILO). Cyclopentane - International Chemical Safety Card (ICSC 0353). 2025, Available online: https://chemicalsafety.ilo.org/dyn/icsc/showcard.display?p_lang=en&p_version=2&p_card_id=0353. [Accessed: 2025-02-25].

[71] NOAA (National Oceanic and Atmospheric Administration). Acetone CAMEO chemicals. 2025, Available online: https://cameochemicals.noaa.gov/chris/ACT.pdf. [Accessed 25 February 2025].

[72] Ochoa GV, Peñaloza CA, Rojas JP. Thermoeconomic modelling and parametric study of a simple ORC for the recovery of waste heat in a 2 MW gas engine under different working fluids. Appl Sci 2019;9(21). http://dx.doi.org/10.3390/app9214526, URL https://www.mdpi.com/2076-3417/9/21/4526.

[73] Ochoa GV, Isaza-Roldan C, Duarte Forero J. Economic and exergo-advance analysis of a waste heat recovery system based on regenerative organic rankine cycle under organic fluids with low global warming potential. Energies 2020;13(6). http://dx.doi.org/10.3390/en13061317.

[74] Klonowicz P, Witanowski Ł, Jędrzejewski Ł, Suchocki T, Lampart P. A turbine based domestic micro ORC system. Energy Procedia 2017;129:923–30. http://dx.doi.org/10.1016/j.egypro.2017.09.112, 4th International Seminar on ORC Power SystemsSeptember 13-15th 2017POLITECNICO DI MILANOBOVISA CAMPUSMILANO, ITALY.

[75] Ferrara F, Gimelli A, Luongo A. Small-scale concentrated solar power (CSP) plant: ORCs comparison for different organic fluids. Energy Procedia 2014;45:217–26. http://dx.doi.org/10.1016/j.egypro.2014.01.024, ATI 2013 - 68th Conference of the Italian Thermal Machines Engineering Association.

[76] Valencia Ochoa G, Cárdenas Gutierrez J, Duarte Forero J. Exergy, economic, and life-cycle assessment of ORC system for waste heat recovery in a natural gas internal combustion engine. Resources 2020;9(1). http://dx.doi.org/10.3390/resources9010002.

[77] Kocaman E, Karakuş C, Yağlı H, Koç Y, Yumrutaş R, Koç A. Pinch point determination and Multi-Objective optimization for working parameters of an ORC by using numerical analyses optimization method. Energy Convers Manage 2022;271:116301. http://dx.doi.org/10.1016/j.enconman.2022.116301.

[78] Herrera-Orozco I, Valencia-Ochoa G, Duarte-Forero J. Exergo-environmental assessment and multi-objective optimization of waste heat recovery systems based on Organic Rankine cycle configurations. J Clean Prod 2021;288:125679. http://dx.doi.org/10.1016/j.jclepro.2020.125679.

[79] Choudhary NK, Karmakar S. Thermoeconomic analysis of organic Rankine cycle with different working fluids for waste heat recovery from a coal-based thermal power plant. J Therm Anal Calorim 2024. http://dx.doi.org/10.1007/s10973-024-13142-3.

[80] Schuster S, Markides CN, White AJ. Design and off-design optimisation of an organic Rankine cycle (ORC) system with an integrated radial turbine model. Appl Therm Eng 2020;174:115192. http://dx.doi.org/10.1016/j.applthermaleng.2020.115192.

[81] Chatzopoulou MA, Lecompte S, Paepe MD, Markides CN. Off-design optimisation of organic Rankine cycle (ORC) engines with different heat exchangers and volumetric expanders in waste heat recovery applications. Appl Energy 2019;253:113442. http://dx.doi.org/10.1016/j.apenergy.2019.113442.

[82] Fatigati F, Vittorini D, Wang Y, Song J, Markides CN, Cipollone R. Design and operational control strategy for optimum off-design performance of an ORC plant for low-grade waste heat recovery. Energies 2020;13(21). http://dx.doi.org/10.3390/en13215846.

[83] Baldi F, Ahlgren F, Nguyen T-V, Thern M, Andersson K. Energy and exergy analysis of a cruise ship. Energies 2018;11(10). http://dx.doi.org/10.3390/en11102508.

[84] Tutunea D, Dumitru I, Racila L, Otat O, Matei L, Geonea I. Characterization of sunflower oil biodiesel as alternative for diesel fuel. In: Burnete N, Varga BO, editors. Proceedings of the 4th international congress of automotive and transport engineering. Springer International Publishing; 2019, p. 172–80. http://dx.doi.org/10.1007/978-3-319-94409-8_21.

[85] Bouman EA, Lindstad E, Rialland AI, Strømman AH. State-of-the-art technologies, measures, and potential for reducing GHG emissions from shipping – A review. Transp Res Part D: Transp Environ 2017;52:408–21. http://dx.doi.org/10.1016/j.trd.2017.03.022.

[86] Baldasso E, Gilormini TJA, Mondejar ME, Andreasen JG, Larsen LK, Fan J, et al. Organic Rankine cycle-based waste heat recovery system combined with thermal energy storage for emission-free power generation on ships during harbor stays. J Clean Prod 2020;271:122394. http://dx.doi.org/10.1016/j.jclepro.2020.122394.

[87] Quoilin S, Broek MVD, Declaye S, Dewallef P, Lemort V. Techno-economic survey of Organic Rankine Cycle (ORC) systems. Renew Sust. Energ Rev 2013;22:168–86. http://dx.doi.org/10.1016/j.rser.2013.01.028.

[88] Girgin I, Ezgi C. Design and thermodynamic and thermoeconomic analysis of an organic Rankine cycle for naval surface ship applications. Energy Convers Manag 2017;148:623–34. http://dx.doi.org/10.1016/j.enconman.2017.06.033.

[89] Lemmens S. Cost engineering techniques and their applicability for cost estimation of organic Rankine cycle systems. Energies 2016;9(7). http://dx.doi.org/10.3390/en9070485.

[90] Cavalcanti EJ, Motta HP. Exergoeconomic analysis of a solar-powered/fuel assisted Rankine cycle for power generation. Energy 2015;88:555–62. http://dx.doi.org/10.1016/j.energy.2015.05.081.

[91] Gomaa MR, Mustafa RJ, Al-Dhaifallah M, Rezk H. A low-grade heat Organic Rankine Cycle driven by hybrid solar collectors and a waste heat recovery system. Energy Rep 2020;6:3425–45. http://dx.doi.org/10.1016/j.egyr.2020.12.011.

[92] Li T, Zhang Y, Gao H, Gao X, Jin F. Techno-economic-environmental performance of different system configuration for combined heating and power based on organic rankine cycle and direct/indirect heating. Renew Energy 2023;219:119553. http://dx.doi.org/10.1016/j.renene.2023.119553.

[93] Mohd Noor C, Noor M, Mamat R. Biodiesel as alternative fuel for marine diesel engine applications: A review. Renew Sust. Energ Rev 2018;94:127–42. http://dx.doi.org/10.1016/j.rser.2018.05.031.

[94] ANAVE (Asociación de navieros españoles). Precio de los combustibles marinos 2020–2024 ($/t). 2024, Available online: https://anave.es/precio-de-los-combustibles-marinos/. [Accessed 21 July 2024].

[95] Baldasso E, Andreasen JG, Mondejar ME, Larsen U, Haglind F. Technical and economic feasibility of organic Rankine cycle-based waste heat recovery systems on feeder ships: Impact of nitrogen oxides emission abatement technologies. Energy Convers Manag 2019;183:577–89. http://dx.doi.org/10.1016/j.enconman.2018.12.114.

[96] Konur O, Yuksel O, Korkmaz SA, Colpan CO, Saatcioglu OY, Muslu I. Thermal design and analysis of an organic rankine cycle system utilizing the main engine and cargo oil pump turbine based waste heats in a large tanker ship. J Clean Prod 2022;368:133230. http://dx.doi.org/10.1016/j.jclepro.2022.133230.

[97] Habibi H, Zoghi M, Chitsaz A, Javaherdeh K, Ayazpour M. Thermo-economic analysis and optimization of combined PERC - ORC - LNG power system for diesel engine waste heat recovery. Energy Convers Manag 2018;173:613–25. http://dx.doi.org/10.1016/j.enconman.2018.08.005.

[98] Shu G, Liu P, Tian H, Wang X, Jing D. Operational profile based thermal-economic analysis on an Organic Rankine cycle using for harvesting marine engine's exhaust waste heat. Energy Convers Manag 2017;146:107–23. http://dx.doi.org/10.1016/j.enconman.2017.04.099.

[99] Wang Z, Chen H, Xia R, Han F, Ji Y, Cai W. Energy, exergy and economy (3E) investigation of a SOFC-GT-ORC waste heat recovery system for green power ships. Therm Sci Eng Prog 2022;32:101342. http://dx.doi.org/10.1016/j.tsep.2022.101342.

[100] Elkafas AG. Thermodynamic analysis and economic assessment of organic Rankine cycle integrated with thermoelectric generator onboard container ship. Processes 2024;12(2). http://dx.doi.org/10.3390/pr12020355.